

Recent Advances of Transition Metal Complexes for Photopolymerization and 3D Printing under Visible Light

Valentina Ferraro, Clara R. Adam, Aleksandra Vranic, and Stefan Bräse*

The possibility of exploiting visible light to induce polymerizations is extremely appealing from a technological point of view as it improves the sustainability of the overall process. To achieve this objective, it is necessary to employ single- or multicomponent systems containing a photoinitiator, and in some cases, a photosensitizer in combination. Due to their long-lived excited states and reversible redox properties, transition metal complexes are a valid choice to be applied in photoinitiating systems, often exhibiting enhanced conversions compared to purely organic compounds. This review presents an overview of the transition metal complexes exploited in photopolymerization reactions. Particular attention will be devoted to recent applications in 3D printing, highlighting the possible challenges that need to be faced to achieve highly efficient and more sustainable processes.

technique that exploits specific wavelengths to generate radicals or cations as initiating species or growing chains.^[2] Unlike traditional thermal processes, the use of light as a chemical energy source allows to perform the reaction at lower temperatures. This aspect is particularly relevant when working with acrylates, methacrylates, and styrenes where high temperatures are required to initiate the polymerization.^[3] The resulting polymer can be used for various applications, from adhesives, dentistry, coatings, and inks, to 3D printing.^[4] Temporal and spatial control should also be mentioned between the advantages together with the possibility of working without any required solvent or work-up, and with high polymerization rates.^[4b,5] Despite being widely applied in photopolymerization reactions, UV light is expensive and energy demanding.

Moreover, UV photons are characterized by low penetration depth, as shown in **Figure 1**, and they can potentially cause cell photodamage and photodegradation of reactants and products.^[4a,6] To improve the overall sustainability of the process and avoid irradiation damage, visible and low-intensity light should be preferred instead of UV light, and this aspect became feasible after the spread of light-emitting diodes (LEDs).

Photopolymerizations require photoinitiators (PIs, see **Table 1** for the full name for each abbreviation) capable of absorbing light and forming free radicals.^[8] The essential prerequisite is that the absorption of the PI and the emission of the light source must intersect, possibly where the molar extinction coefficient of the former is high. In Norrish Type I PIs like bisacylphosphine oxides (e.g. BAPO or Irgacure 819, see **OC-1** in **Scheme 1**) or organometallic compounds such as titanocene and metal carbonyl compounds, the radicals are formed via homolytic α -cleavage of bonds in the PIs. If the absorption properties of the PI do not perfectly match the emissive features of the light source, it is possible to introduce photosensitizers (PSs) that can transfer the excitation to the PI. Sometimes only one PI is insufficient to perform an efficient photopolymerization; therefore, a co-initiator is introduced in the reaction media. In two-component systems (Norrish Type II), the active species are generated by energy, electron, or hydrogen atom transfer or by photoinduced cleavage of bonds via electron transfer between a PI and a co-initiator or a PS and a PI. As shown in **Scheme 2**, the initiation mechanism can be photoreducible or photooxidative. By light absorption, the PI gets excited and can react with an electron acceptor A (e.g. iodonium salts or alkyl halides) or with an


1. Introduction

Visible light is widely exploited to induce chemical transformations and represents one of the cheapest and most sustainable reactants a chemist can use. Therefore, in recent years the interest in greener processes determined the spread of photochemistry, allowing the performance of chemical reactions under light irradiation and in mild conditions.^[1] In photochemistry, photopolymerization or photoinitiated polymerization represents a

V. Ferraro, C. R. Adam, A. Vranic, S. Bräse
Institute of Organic Chemistry (IOC)
Karlsruhe Institute of Technology (KIT)
Fritz-Haber-Weg 6, 76131 Karlsruhe, Germany
E-mail: braese@kit.edu

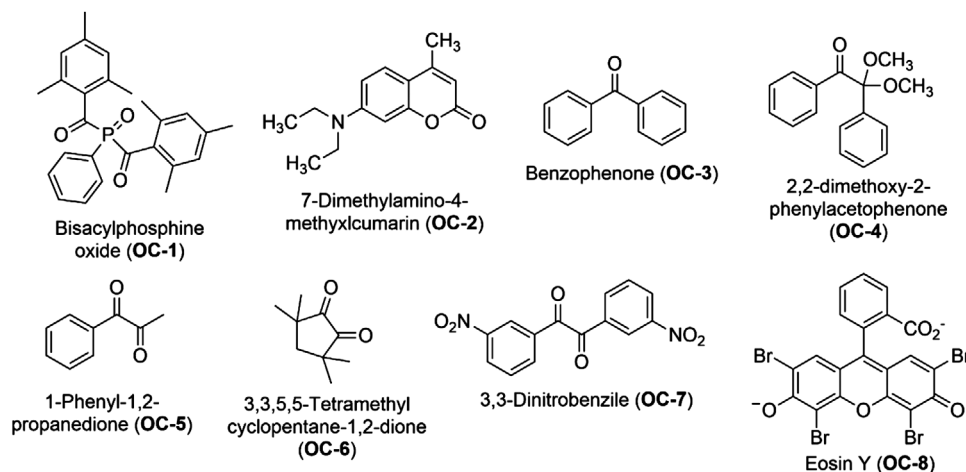
V. Ferraro, C. R. Adam, A. Vranic, S. Bräse
3DMM2O—Cluster of Excellence (EXC-2082/1–390761711)
KIT
Fritz-Haber-Weg 6, 76131 Karlsruhe, Germany

S. Bräse
Institute of Biological and Chemical Systems—Functional Molecular Systems (IBCS-FMS)
KIT
Hermann-von-Helmholtz-Platz 1, 76344 Eggenstein-Leopoldshafen, Germany

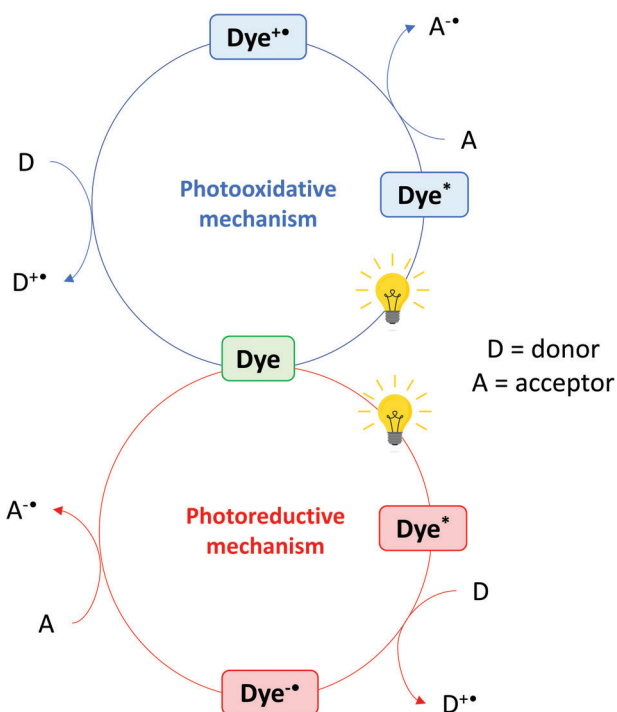
 The ORCID identification number(s) for the author(s) of this article can be found under <https://doi.org/10.1002/adfm.202302157>

© 2023 The Authors. Advanced Functional Materials published by Wiley-VCH GmbH. This is an open access article under the terms of the Creative Commons Attribution License, which permits use, distribution and reproduction in any medium, provided the original work is properly cited.

DOI: 10.1002/adfm.202302157



Scheme 1. Selected organic compounds applied as PIs for 3D printing (see Table 1 for the full names of the mentioned abbreviations).^[4a,10]



Scheme 2. Photoinduced electron transfer in photoinitiating systems, here indicated as “dye” for simplicity (A = acceptor, D = donor).

electron/hydrogen donor D (e.g. amines or silanes) to generate the active species that initiate the photopolymerization. Coumarin and keto-coumarin derivatives (OC-2 in Scheme 1) or ketone-based systems (OC-3 to OC-7 in Scheme 1) are commonly employed as Norrish Type II PIs. On the other hand, multicomponent systems are normally composed of a PS and a PI in combination with a molecule able to enhance the efficiency through side-reactions, such as eosin (OC-8 in Scheme 1)/amine/onium salt or Ir(III)/onium salt (or *N*-vinyl carbazole, NVC)/silane.^[9]

A wide variety of PIs and PSs were designed and successfully applied to photopolymerization, and they can roughly be divided into organic compounds and transition metal complexes. The

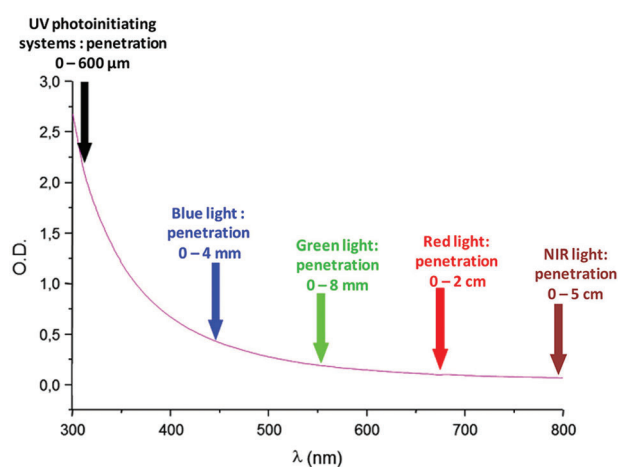


Figure 1. Light penetration inside polystyrene latex (112 nm of average diameter) and calculated penetrations of selected photons. Reproduced with permission.^[7] Copyright 2018, American Chemical Society.

former can be efficiently used for such purposes, but they are normally characterized by lower extinction coefficients and absorptions below 400 nm.^[11] Instead, in more recent years, owing to their redox potentials and long photoluminescent lifetimes which allow them to take part in electron transfer reactions,^[12] transition metal complexes emerged as possible candidates to be used in photoinitiating systems, sometimes exhibiting enhanced conversions in comparison to organic dyes.^[4a]

In the following pages, we will discuss the state of the art concerning transition metal complexes applied in photoinitiating systems, with a precise focus dedicated to their application in the emerging field of 3D printing.

2. Principles of Photopolymerization

Photopolymerizations can be roughly divided into photoinitiated and photocontrolled reactions. In the former, the propagating species is generated upon excitation of a PI, while the polymerization proceeds chemically or thermally. On the contrary, in the

Table 1. Full names and abbreviations used in the review.

| Full name | Abbreviation |
|--|--------------|
| 4-Chlorostyrene | 4-Cl-St |
| 4-Methoxystyrene | 4-OMe-St |
| Acrylic acid | AA |
| Acrylamide | AM |
| Atom transfer radical polymerization | ATRP |
| <i>n</i> -Butyl acrylate | <i>n</i> BA |
| Bisacrylphosphine oxide (Irgacure 819) | BAPO |
| Benzyl bromide | BB |
| 2,6-Di- <i>tert</i> -butyl-4-methylphenol | BHT |
| Bisphenol A-glycidyl methacrylate | BisGMA |
| 2-(<i>n</i> -butyltrithiocarbonate)propionic acid | BTPA |
| 9 <i>H</i> -Carbazole-9-ethanol | CARET |
| 4-Cyano-4-[(dodecylsulfanylthiocarbonyl)sulfanyl]pentanoic acid | CDTPA |
| Continuous liquid interface production | CLIP |
| 4-Cyano-4-(phenylcarbonothioylthio)pentanoic acid | CPADB |
| Chain transfer agent | CTA |
| Diethylene glycol divinyl ether | DDE |
| Diethyl bromomalonate | DEBrM |
| <i>N,N</i> -Diisopropylethylamine | DIPEA |
| <i>N,N</i> -Dimethylacrylamide | DMA |
| 2,2-Dimethoxy-2-phenylacetophenone | DMPA |
| <i>N,N</i> -Dimethyl- <i>p</i> -toluidine | DMPT |
| Digital light processing | DLP |
| Direct laser writing | DLW |
| Tri(ethylene glycol) divinyl ether | DVE-3 |
| Ethyl α -bromoisobutyrate | EBiB |
| Ethyl α -bromophenylacetate | EBPA |
| Ethyl 4-(dimethylamino)benzoate | EDB |
| 2-(2,4,5,7-tetrabromo-6-oxido-3-oxo-3 <i>H</i> -xanthen-9-yl)benzoate | Eosin Y |
| (3,4-Epoxy-cyclohexane)methyl 3,4-epoxycyclohexanecarboxylate | EPOX |
| Free radical polymerization | FRP |
| Gelatin-methacryol | GelMA |
| Isobutyl vinyl ether | IBVE |
| isosorbide diglycidyl ether | IDE |
| Bis(4- <i>tert</i> -butylphenyl)iodonium (Speedcure 938 as hexafluorophosphate salt) | Iod |
| [Methyl-4-phenyl(methyl-1-ethyl)-4-phenyl]iodonium tetrakis(pentafluorophenyl)borate | Iod1 |

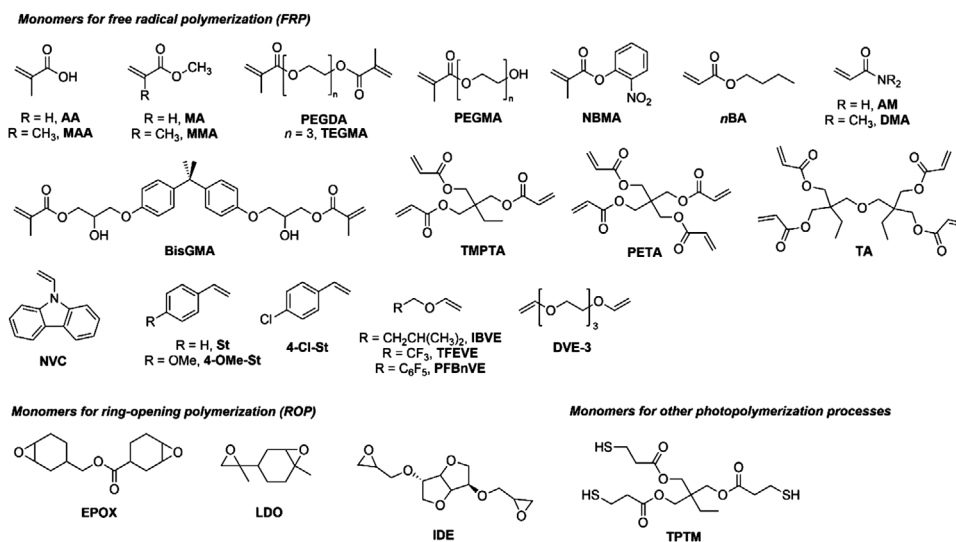
(Continued)

Table 1. (Continued).

| Full name | Abbreviation |
|--|--------------|
| Interpenetrated polymer network | IPN |
| Isopropylthioxanthone | ITX |
| Limonene dioxide | LDO |
| Light-emitting diode | LED |
| Methacrylate | MA |
| Methacrylic acid | MAA |
| <i>N</i> -Methyl- <i>N,N</i> -diethanolamine | MDEA |
| Metal-to-ligand charge transfer | MLCT |
| Methyl methacrylate | MMA |
| <i>o</i> -Nitrobenzyl methacrylate | NBMA |
| <i>N</i> -Phenylglycine | NPG |
| <i>N</i> -Vinylcarbazole | NVC |
| Organic light-emitting diode | OLED |
| Phenacyl bromide | PABr |
| Photoinitiator | PI |
| Photosensitizer | PS |
| Pentaerythritol tetraacrylate | PETA |
| Photoinduced electron transfer – reversible addition-fragmentation chain transfer | PET-RAFT |
| Poly(ethylene glycol) diacrylate | PEGDA |
| Poly(ethylene glycol) methacrylate | PEGMA |
| Pentafluorobenzyl vinyl ether | PFBnVE |
| Trisodium (8 <i>Z</i>)-7-oxo-8-[(4-sulfonatophthalen-1-yl)hydrazinylidene]naphthalene-1,3-disulfonate | Ponceau 4R |
| Ring-opening polymerization | ROP |
| Stereolithography | SLA |
| Styrene | St |
| Di(trimethylolpropane) tetraacrylate | TA |
| Thermally activated delayed fluorescence | TADF |
| Triethylamine | TEA |
| Triethylene glycol dimethacrylate | TEGDMA |
| 2,2,6,6-Tetramethylpiperidine-1-oxyl | TEMPO |
| 2,2,2-Trifluoroethyl vinyl ether | TFEVE |
| Trimethylolpropane triacrylate | TMTPA |
| Trimethylolpropane tris(3-mercaptopropionate) | TPTM |
| Tris(trimethylsilyl)silane | TTMSS |

latter, both initiation and propagation processes are governed by light. Thus, the polymerization can be spatially and temporally controlled and, consequently, properties like molecular weight, architecture, and tacticity.^[13]

Depending on the mechanism, it is possible to distinguish radical and cationic photopolymerization. In free radical photopolymerization (FRP), the PI at the excited state can directly



Scheme 3. Selected monomers applied for photopolymerization (see Table 1 for the full names of the mentioned abbreviations).

generate the radical active species that initiate the polymerization, as occurs for instance with acrylic acid in the presence of triphenylphosphine and derivatives.^[14] The monomers employed in FRP are normally vinylic substrates, mostly acrylates, such as trimethylolpropane triacrylate (TMPTA). On the other hand, cationic polymerization is normally more versatile than FRP because the process is initiated by the photolysis of a cationic PI that generates a protonic or a Lewis acid. Then, the polymerization proceeds through ring-opening (ROP) or double bond activation reaction. Epoxides, cyclic ethers, and acetals can be used as possible monomers as well as acrylates.^[15] Selected monomers applied for light induced FRP and ROP are sketched in **Scheme 3**. Moisture can inhibit cationic polymerization reactions because water can attack the oxonium cation and stop the growth of the chain,^[16] but the presence of oxygen does not influence the process as it occurs instead for FRP, and once the active cations are formed, the process continues even without a light source. Instead, FRP often requires light to proceed, since in dark conditions the reaction is significantly slowed down by the negligible presence of active radicals.^[17] Cationic PIs can act in direct or indirect mode depending on whether the active species is formed by photolysis of the PIs or by electron transfer reaction between PIs and active cations. Hybrid photopolymerization, based on the free radical and cationic processes, was invented to combine the advantages of both techniques, i.e. reduced inhibition related to the presence of oxygen and moisture, higher polymerization rates, and best mechanical and physical properties in the final product. In the initiating process, cations and free radicals exist simultaneously in the reaction media because the latter generates the former.^[15] The PIs and additives discussed in the following pages are depicted in **Scheme 4** (see Table 1 for the full names and corresponding abbreviations).

3. 3D Printing and Challenges

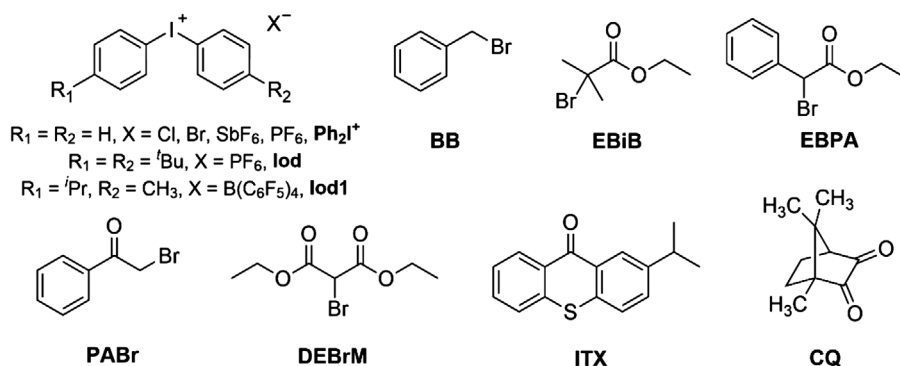
The following chapter describes the basic concepts of 3D printing and issues its existing challenges. The technique behind 3D printing, also known as additive manufacturing,^[18] allows the

creation of large and complex functional architectures by assembling small building blocks called “voxels”, which are 3D volume elements comparable to pixels in 2D pictures. The smaller the voxel is, the more precise 3D structures can be printed. Voxels from the size of several hundreds of μm to 100 nm and printing rates of 10^7 voxels per second have been reported lately.^[19] When the manufacture of 3D structures is done by light irradiation, the underlying process relies on photopolymerization-based techniques such as stereolithography (SLA), digital light processing (DLP) and continuous liquid interface production (CLIP). These techniques combine high printing speed with low costs and flexibility in the design of the photoresists. In SLA, a movable photon source is used to initiate the photopolymerization and print solid layers on top of each other with a point-by-point exposure. Instead, during DLP all the layers are exposed to the light source at the same time. The advantages of DLP include reduced printing times and low consumption of photoresists, since the light source irradiates the bottom of the resist, and the building platform is dipped into it from above. In this way, the printed layer is not directly in contact with air, limiting oxygen inhibition. For the same purpose, with CLIP an oxygen-permeable window is introduced to form a layer where radical photopolymerization is inhibited, thus enabling fast printing speeds.^[4a,20]

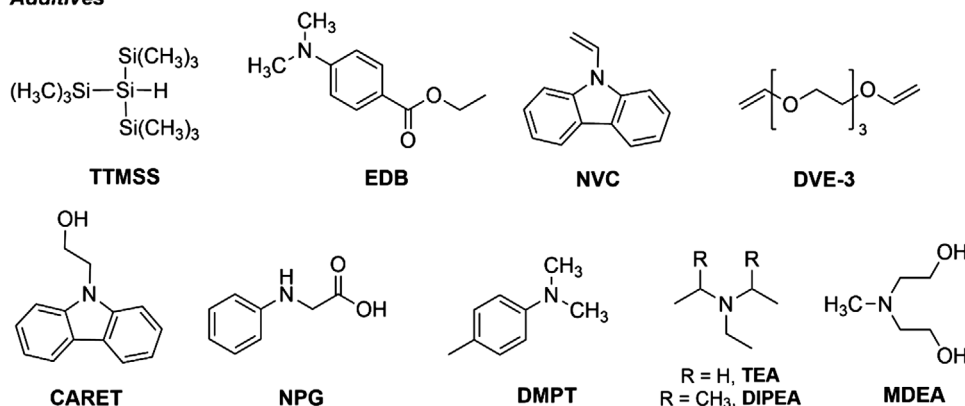
Several organic PIs (see Scheme 1) have been successfully employed for 3D printing via light induced polymerization. However, some issues are often encountered, such as air sensitivity due to their tendency to oxidize or form peroxides. As previously stated, molecular oxygen can quench the excited state of the PI and prevent the generation of radicals.^[4a,21] Besides with DLP and CLIP, this issue can be solved by working under inert gas, such as nitrogen or argon, or by covering the surface with liquid wax to achieve an oxygen-free environment.^[22] Even so, not all 3D printing equipment is suitable for this procedure which is also costly, and a cheaper solution is represented by working in laminate, as it will be further detailed below.

In contrast, among the disadvantages, one of the biggest hurdles of these photopolymerization techniques is related to the formation of radicals. Commercial 3D printers use irradiation

Photoinitiators



Additives



Scheme 4. PIs and additives commonly applied in photoinitiating systems (see Table 1 for the full names of the mentioned abbreviations).

between 365 and 405 nm,^[23] but photoinitiating systems that work with visible light are rare compared to blue/UV light systems currently exploited for 3D printing.^[20] Visible light sources have the advantage of being eco-friendly in terms of energy efficiency and do not release ozone by reaction with molecular dioxygen while having low thermal effects and long operating lifetimes. However, irradiation sources with longer wavelengths, such as NIR, are more benign for living cells and should be preferred for biomedical applications.^[4a] A possible way to exploit these low energy irradiation wavelengths relies on two-photon absorption, a non-linear absorption process predicted by Maria Göppert-Mayer in 1931,^[24] that was recently applied to 3D printing using metal-free PIs.^[25] When a photon of a specific wavelength gets absorbed by the PI, it transits from the ground state into a higher energetic excited state. This process can be achieved using a single photon or by subsequent absorption of a second photon. According to the latter mechanism, the absorption of a single photon is insufficient to reach an excited state, but the process can take place with the almost simultaneous absorption of two photons. With the first photon, an electron passes from the ground state into a temporarily existing intermediate state with a short lifetime. This is seen as a virtual state as it exists only during irradiation. The molecule subsequently passes into the excited state with the help of a second photon. The mechanism of one- and two-photon absorption is shown in the Jablonski diagram in **Figure 2**. A schematic illustration of a complete photopolymer-

ization with the excitation of one or two photons is displayed in **Scheme 5**.

The formation of radicals $R\bullet$ starts when the PI reaches the excited state, but the energy must be higher than the energy of the involved breaking bond.^[24] Nevertheless, it should be considered that this ideal mechanism is often disturbed by different undesirable side reactions, whose probability of happening is sometimes higher than the generation of the radicals.^[26] In particular, aromatic triplet-state ketones (**OC-3** and **OC-4** in Scheme 1) and diketones (**OC-5** to **OC-7** in Scheme 1) are especially likely to undergo hydrogen abstraction.^[27] One strategy adopted to minimize this process involves the use of radical scavengers, such as 2,2,6,6-tetramethylpiperidinyl-1-oxyl (TEMPO), which acts like a hydrogen abstractor and hydrogen atom transfer catalyst. By adding TEMPO to a photore-sist consisting of a PI and a monomer, hydrogen abstraction can be suppressed by lowering the lifetime of the intermediate state.^[10,28]

The photopolymerization obtained with two-photon absorption permitted to reduce the dimension of the voxels between a few μm and hundreds of nm, moving from 3D printing to 3D nano-printing.^[29] Consequently, the 3D printed objects could be employed for a wide variety of applications that include micromachines,^[30] microfluidic devices^[31] and tissue engineering scaffolds,^[32] that could not be prepared with common one-photon 3D printing techniques.^[33] For instance, PIs such as

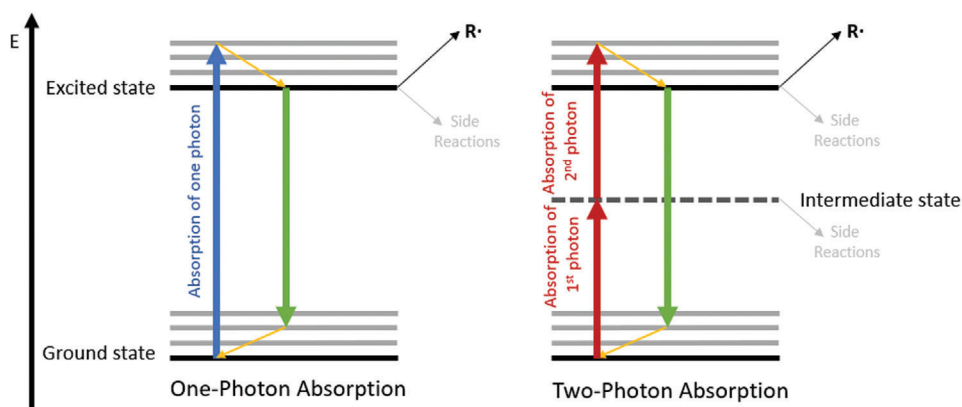
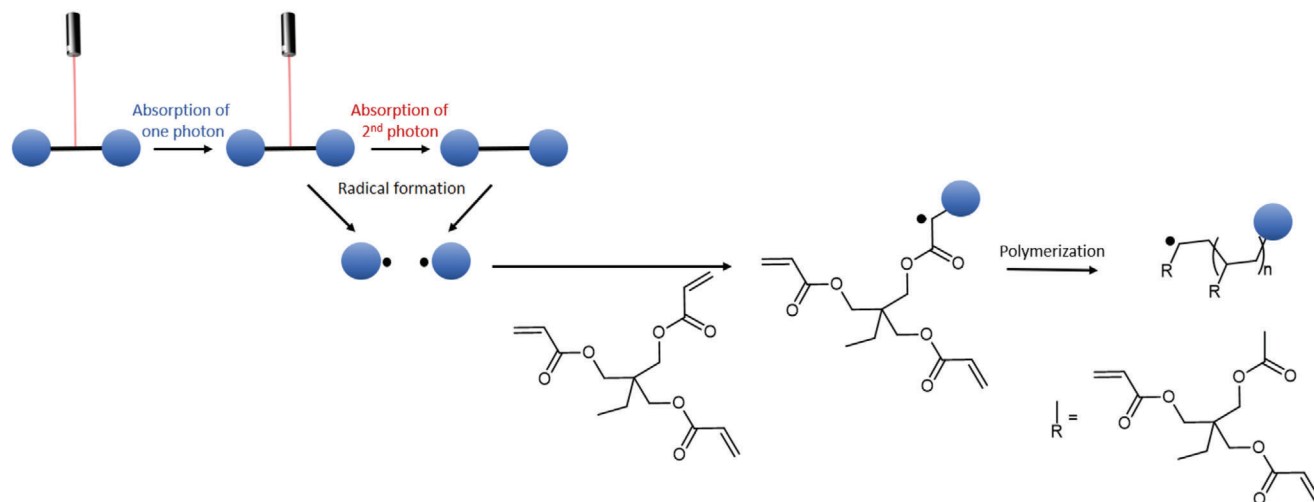


Figure 2. Jablonski diagram for one-photon (left) and two-photon (right) absorption. In the case of one-photon absorption, a single photon is excited from the ground state directly to an excited state with higher energy. Two-photon absorption happens by the subsequent absorption of one photon from the ground state to a short-lived virtual intermediate state, followed by the absorption of a second photon into the excited state. Different side reactions can occur next to the desired radical formation at the excited and intermediate states.



Scheme 5. During photopolymerization, the formation of the radicals starts either after the absorption of a single photon or after the absorption of a second photon. The radical adds to the monomer (TMPTA) and starts a polymerization process.

OC-5, OC-6 and OC-7 lead to structures in the size of 2 μm in two-photon absorption-based 3D printing,^[10] while using OC-8 in SLA 2-mm-wide structures were obtained.^[20]

Despite all the advantages presented before, the light source still represents a challenge in 3D printing, both in one-photon and two-photon absorption processes, since only specific irradiation wavelengths are available. For many PIs, photons can be absorbed in either or both wavelengths, but there are also molecules for which no polymerization is observable at either wavelength, thus potentially excluding them as PIs. Furthermore, it is also worth mentioning that the light source is characterized by a certain power range, which is not always sufficient to break the chemical bond and generate radicals.^[26] As a matter of fact, the application of two-photon absorption photopolymerization is still limited by the light intensity required which is normally between 10^1 and 10^6 W cm^{-2} ,^[33,34] although higher values of $10^{12} \text{ W cm}^{-2}$ were also reported.^[29] This aspect is still a challenge for two-photon absorption 3D printing and prevents its application with LEDs, whose light intensity is $\approx 10^2 \text{ W cm}^{-2}$.^[25]

4. Metal-Based Photoinitiating Systems

The transition metal complexes described in the following pages act as PIs or PSs. As concerns the former, organometallic complexes exhibit lower bond energy compared to organic compounds (see Table 2), meaning that the metal-carbon bond can easily be broken by light irradiation and thus they can be employed as PIs.^[35] The organometallic compounds employed as PIs contain soft σ -donor ligands such as the cyclopentadienyl anion (Cp^-), or π -acceptors such as carbon monoxide (CO). In the latter case, the metal center is typically in zero-valent oxidation state. The application of metal carbonyl derivatives and metallocenes as PIs for photopolymerization was reported back in the Sixties due to their ability to generate radicals once directly exposed to light irradiation originated from a 500 W Xenon lamp, or from a 125 W high-pressure Hg lamp filtered to give pure monochromatic light centered at 436 nm.^[36]

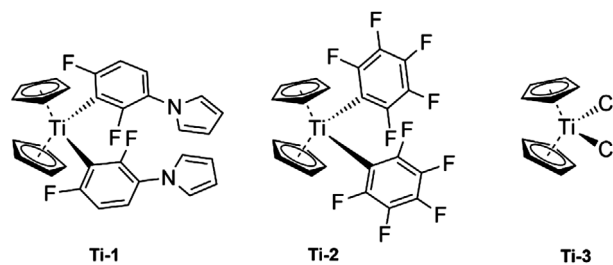
In contrast, the use of visible light for photoredox catalysis was developed in the late 2000s, and even later, it was applied to

Table 2. Selected bond energies of carbon with heteroatoms and different metals with carbon, carbonyl, cyclopentadiene, and arene^[35].

| Bond | Bond energy [kJ mol ⁻¹] |
|----------------------------------|--|
| C–C | 345 |
| C=C | 615 |
| C–O | 358 |
| C=O | 708 |
| C–N | 305 |
| C=N | 892 |
| Ti–Cp ^{a)} | 318 |
| Ti–C | 432 |
| Cr–CO | 105 |
| | 340 |
| Cr–C ₆ H ₆ | 403 |
| Mo–Cp ^{a)} | 149 |
| Mo–CO | 179 |
| Re–CO | 350 |
| Fe–Cp ^{a)} | 116 |
| Fe–CO | 122 |
| Ir–C | 430 |
| Pd–C | 606 |
| Pt–C | 606 |

^{a)} Cp = cyclopentadienyl anion

macromolecules and polymers after the spread of blue LEDs that could be used as light sources.^[17b,37] Due to their intense light absorptions, photoactive transition metal complexes are suitable candidates to be employed as PSs in photoinitiating systems. As it will be further discussed in detail, PSs are normally characterized by extended π -conjugated ligands, such as polypyridines like 2,2'-bipyridine (bpy) and 1,10-phenanthroline (phen), or porphyrins. In some cases, aromatic phosphines are also employed as soft σ -donor ligands, for instance in Cu(I) complexes. The photoluminescent properties are normally originated by charge transfer excited states such as metal-to-ligand charge processes (MLCT) as observable in Fe(II), Ru(II), Ir(III) and Cu(I) derivatives. Differently from PIs, that normally do not exhibit photoluminescent properties, the involvement of long-lived triplet emitting states in PSs can improve the production of reactive species by electron transfer.^[12] In addition, adapted redox potentials, and reversible oxidation and reduction processes can enhance the polymerization process by acting on the rate of interaction between photocatalysts and additives.^[38] The investigation of metal-based photoinitiating systems for photopolymerization under visible light was first developed by Lalevéé and coworkers that tested [Ru(bpy)₃]²⁺ as PS back in 2010, in combination with Ph₂I⁺ as PI and TTMSS as additive. At the excited state, [Ru(bpy)₃]^{2+*} can decompose Ph₂I⁺ by photochemical induced electron transfer to generate a Ph•, thus initiating the polymerization. Different light sources were employed, including a green fluorescent bulb ($I = 18 \text{ mW cm}^{-2}$, kept at 4 cm distance), a 150 W Xenon lamp (filtered for $\lambda > 390 \text{ nm}$, $I \approx 60 \text{ W cm}^{-2}$ in the 360–



Scheme 6. Group IV metal complexes applied in photopolymerizations.

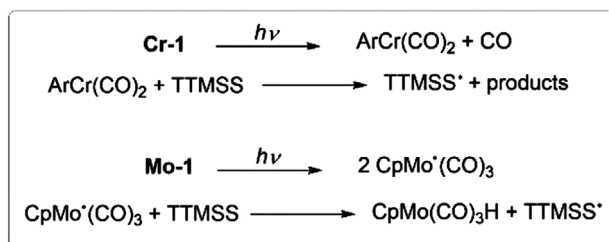
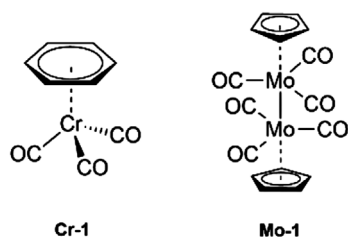
800 nm range), and laser diodes centered at 405, 457, 473, and 532 nm ($I = 100 \text{ mW cm}^{-2}$).^[39] The majority of luminescent transition metal complexes applied as PSs in photoinitiating systems are currently based on precious and rare d⁶ metal centers such as Ru(II) and Ir(III). However, due to their toxicity, high costs, and low abundance, growing interest in earth-abundant transition metal complexes, such as Cu(I) and Fe(II), has spread in recent years. In the following pages, the transition metal complexes investigated will be discussed and sorted by periodic table group.

4.1. Group IV Metal Complexes

The first complexes tested as PIs for ATRP were titanocene and zirconocene due to the combination of lower toxicity, thermal stability, and broad absorptions up to 500 nm. Despite being widely known for the polymerization of α -olefins,^[40] the polymerization of vinyl substrates is not observable without light irradiation.^[36a] As regards Ti(IV) derivatives, bis(cyclopentadienyl)bis[2,6-difluoro-3-(1-pyrrolyl)phenyl]titanocene (Irgacure 784, **Ti-1**) and bis(pentafluorophenyl)titanocene (**Ti-2**), depicted in **Scheme 6**, were efficiently applied for the photopolymerization of acrylates, like TEGDMA.^[21,41] **Ti-1** can also be applied for ROP of EPOX in the presence of TTMSS and Ph₂I⁺ hexafluorophosphate (respectively 0.1%/5%/1% w/w) with a laser diode centered at 405 nm. In the absence of TTMSS, no reaction was observed. Similar results were achieved using the analogous three-component system with **Ti-3** (1%/3%/2% w/w). Complete conversion (<30% in the absence of TTMSS) was obtained under air after 800 s with $\lambda > 400 \text{ nm}$ originating from Xe lamps, diode lasers, or household LED bulbs.^[42]

4.2. Group VI Metal Complexes

Among group VI metals, **Cr-1** and **Mo-1** depicted in **Scheme 7** were described in the literature to be able to initiate photopolymerization reactions.^[21] Dimeric metal-carbonyl derivatives produce radicals after irradiation via metal-metal bond cleavage (**Mo-1** generates CpMo(CO)₃•, Cp⁻ = cyclopentadienyl anion). Instead, with **Cr-1**, ArCr(CO)₂ (Ar = benzene) is obtained after irradiation at 330 nm due to the loss of a CO molecule. A 150 W Xe-Hg lamp ($I \approx 22 \text{ mW cm}^{-2}$ in the 300–400 nm range), a 150 W Xe lamp (filtered for $\lambda > 390 \text{ nm}$; $I \approx 60 \text{ mW cm}^{-2}$ in the 390–800 nm range), and laser diodes at 405 nm ($I \approx 12 \text{ mW cm}^{-2}$), 457 nm, 473 nm, and 532 nm ($I \approx 100 \text{ mW cm}^{-2}$) were employed as light sources. As highlighted in **Scheme 7**, the two active species can



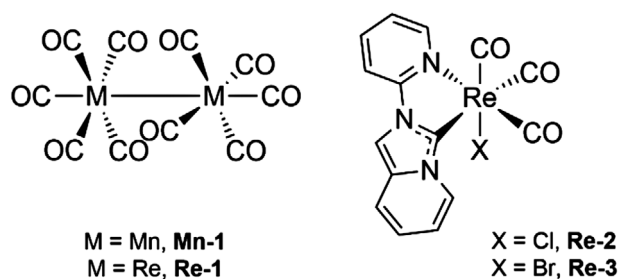
Scheme 7. Group VI metal complexes and photopolymerization mechanism (see Table 1 for the full names of the mentioned abbreviations).

then react with TTMSS and generate the tris(trimethylsilyl)silyl radical to continue the polymerization.^[43]

The interaction between the radical species and TTMSS is quite poor in both cases (hydrogen abstraction rate constant $< 3 \cdot 10^5 \text{ M}^{-1} \text{ s}^{-1}$ for **Cr-1** and $< 2 \cdot 10^5 \text{ M}^{-1} \text{ s}^{-1}$ for **Mo-1**), determining low polymerization rates for the FRP of TMPTA. The presence of TTMSS improves the polymerization but it is not sufficient to obtain an efficient process also because of the slow addition rate constant of the radicals to the monomer and the detrimental presence of oxygen. In fact, the reaction of radicals with oxygen is favored, being characterized by a rate constant $\approx 3 \cdot 10^9 \text{ M}^{-1} \text{ s}^{-1}$, close to the diffusion limit.^[43] The generated radicals $\text{R}\bullet$ react with O_2 to form the weak propagating $\text{RO}_2\bullet$ species via scavenging reaction. On the other hand, TTMSS is frequently used in photoinitiating systems because it reacts to form silicon radicals capable of initiating the photopolymerization. Moreover, this silane can partially reduce oxygen inhibition due to its strong hydrogen donating properties. TTMSS can react with $\text{RO}_2\bullet$ species via hydrogen abstraction to form new active silicon radicals.^[21] Differently from **Cr-1** which was not active toward the ROP, it was possible to obtain over 40% of conversion of EPOX after 400 s of irradiation and with a Xe lamp ($\lambda > 400 \text{ nm}$) in the three-component system **Mo-1**/TTMSS/ Ph_2I^+ (1%/3%/1% w/w). Without TTMSS, the conversion was below 5% under the same experimental conditions.^[43]

4.3. Group VII Metal Complexes

Due to technetium's radioactivity and low abundance, the examples of group VII metal complexes applied for photopolymerization are limited to manganese and rhenium. For the former, the first study regarding the homolytic decomposition of **Mn-1** (see **Scheme 8**) by irradiation with visible light (400–500 nm) or solar irradiation and its possible use to initiate FRP was reported back in the Sixties by Bamford and coworkers.^[36b,c] Similar to what was previously described for **Mo-1**, **Mn-1** generates the active radical species $[\text{Mn}(\text{CO})_5]\bullet$ by metal-metal bond cleavage. The radicals



Scheme 8. Group VII metal complexes applied in photopolymerizations.

are then formed by halogen abstraction from alkyl halides like CCl_4 that can reduce CuBr_2 to CuBr , which is the genuine activator for the ATRP of MMA, MA, and St.^[44] **Mn-1** and the analogous $\text{Re}(0)$ derivative **Re-1** work as Norrish Type II PIs for the ATRP of TMPTA in the presence of TTMSS (1%/3% w/w) and under laser diode at 405 nm or Xe lamp irradiation. Conversions increased up to ten times in the presence of TTMSS compared to the complexes alone (1% w/w). The same complexes were also active toward the photopolymerization of EPOX in the presence of Ph_2I^+ and TTMSS (**Mn-1** or **Re-1**/TTMSS/ Ph_2I^+ , 1%/3%/1% w/w). As previously observed, adding TTMSS is crucial to obtain conversions $\approx 60\%$ for **Mn-1**, and higher polymerization rates compared to the same system with **Ti-3** were observed. In contrast, for **Re-1** no polymerization was observed, even with TTMSS.^[45]

Recently, the first examples of PIs based on $\text{Re}(\text{I})$ -NHC complexes (NHC = N-heterocycle carbene), **Re-2** and **Re-3** were reported by Lalevée et al. and applied in 3D and 4D printing under LED@405 nm. The PIs were tested in a three-component system together with bis-(4-t-butylphenyl)-iodonium hexafluorophosphate (Iod) and ethyl-4-(dimethylamino) benzoate (EDB) for the photopolymerization of poly(ethyleneglycol) diacrylate (PEGDA) monomers. The best performances were achieved using **Re-2** or **Re-3**/Iod/EDB (0.1%/1.5%/1.5% w/w) and were successfully tested for direct 3D laser writing experiments affording the patterns reported in **Figure 3**. The resulting polymers exhibited reversible shape memory in response to temperature and water that were exploited for 4D printing by subsequent swelling and dehydration processes, as shown in **Figure 4**. Both thermal and water responses depended upon the light irradiation time and consequently upon the PEGDA degree of polymerization.^[46]

4.4. Group VIII Metal Complexes

Regarding group VIII metals, $\text{Fe}(\text{II})$ complexes, such as ferrocene (**Fe-1**, **Scheme 9**) and its derivatives, were widely investigated as PIs for FRP of TMPTA and ROP of EPOX. Working on the substituents on the cyclopentadienyl ring, it was possible to tune the absorption properties from 405 to 785 nm, thus increasing the light penetration inside the resins (see **Figure 1**).^[41a,47]

Similarly to what was previously observed for **Mn-1** and **Cr-1**, after irradiation with UV light, the carbonyl iron dimers **Fe-2** and **Fe-3** can decompose homolytically or lose one coordinated CO molecule with the formation of $\text{CpFe}(\text{CO})_2\bullet$ and $\text{Fe}(\text{CO})_8$. The two active species can then react with TTMSS to initiate both FRP of TMPTA and ROP of EPOX, achieving conversions up to 50% after 400 s in three-component systems together with

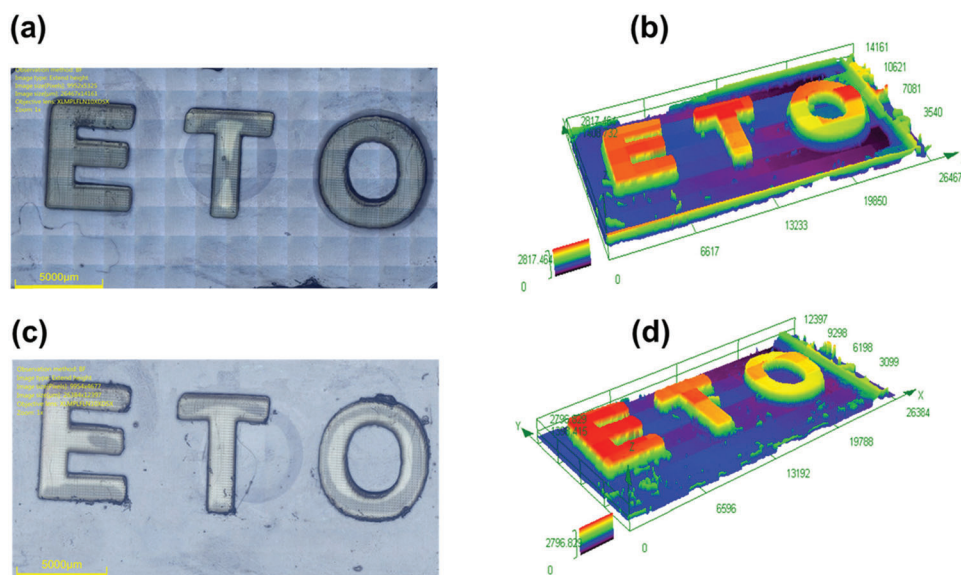


Figure 3. 2D view morphology A,C) and colorful height profile appearance B,D) of the 3D printed patterns obtained through FRP for laser writing experiments of PEGDA and **Re-2** or **Re-3**/Iod/EDB system (see Table 1 for the full names of the mentioned abbreviations). Reproduced with permission.^[46] Copyright 2021, American Chemical Society.

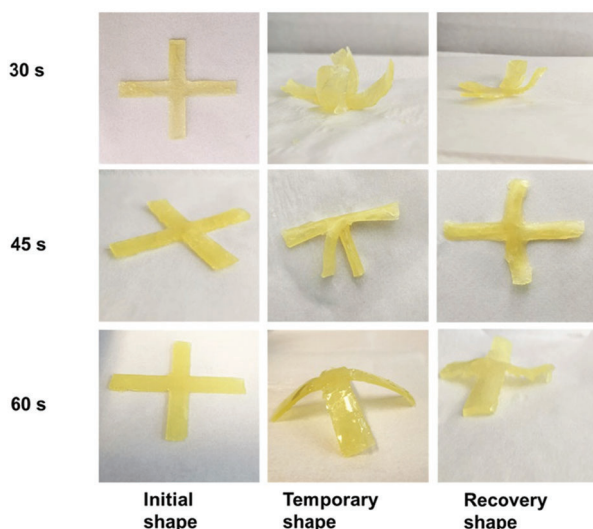
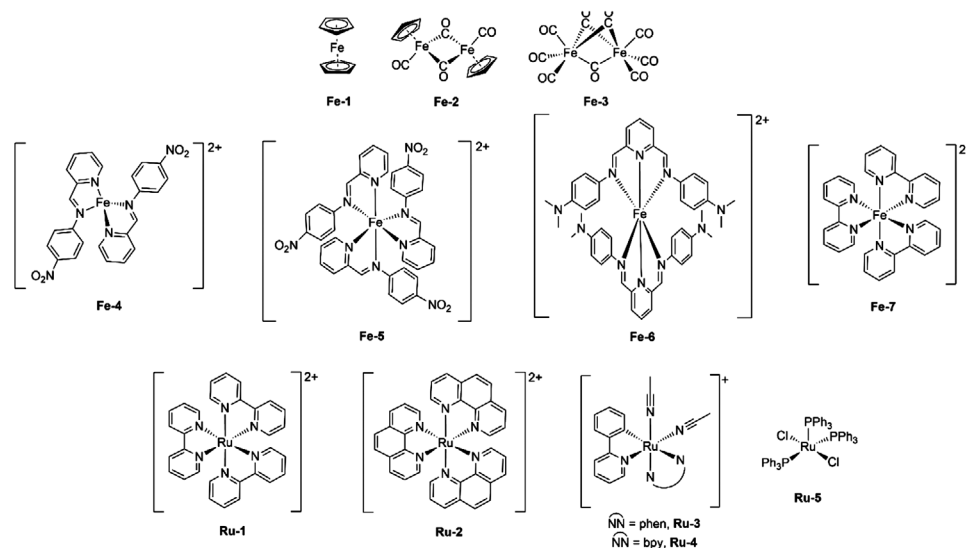


Figure 4. Shape-memory effect of a PEGDA cross for the different light exposure times obtained with **Re-2**/Iod/EDB system at 405 nm (see Table 1 for the full names of the mentioned abbreviations). Adapted with permission.^[46] Copyright 2021, American Chemical Society.

Ph_2I^+ (**Fe-2**: 0.2%/3%/1%; **Fe-3**: 1%/3%/1% w/w). Instead, in the absence of the silane derivative, conversions were always under 10%.^[43] Recently, **Fe-2** was applied as PI for free radical-promoted cationic reversible addition-fragmentation transfer (RAFT) polymerization of vinyl ethers and “living” 3D printing. The complex was tested in combination with dithiocarbamate as a chain transfer agent (CTA) and Ph_2I^+ with different anions, highlighting the influence of their nucleophilicity on the polymerization rate. In fact, besides helping the solubilization of the onium salts, Cl^- and Br^- are strong nucleophiles and thus help to termi-

nate cationic polymerization processes. Owing to its broad absorptions, **Fe-2** was tested with different wavelengths spreading from UV to NIR irradiation in combination with Ph_2I^+ hexafluorophosphate, affording conversion of isobutyl vinyl ether (IBVE) over 97% in all cases after four to six minutes of light exposure. This system was applied to single-layer 3D printing using diethylene glycol divinyl ether (DDE) as monomer and NIR irradiation, affording objects of different thicknesses (1, 4, or 8 mm) depending on the height of the solution (see **Figure 5**).^[48]

Using metal carbonyl complexes in photoinitiating systems is complicated because of their volatility, severe toxicity, and instability; therefore, safer alternatives are highly desirable. In this context, the versatility of iron complexes and their ability to work in oxidative and reductive environments allowed the preparation of a wide variety of derivatives tested toward photopolymerization. Between them, Schiff base homoleptic Fe(II) complexes **Fe-4** and **Fe-5** should be mentioned since they exhibit comparable performances to that of bisacylphosphine oxide (BAPO, OC-1 in Scheme 1) in FRP of TMPTA in laminate and under 405 nm irradiation. The photopolymerization was carried out in three-component systems using low loadings of metal complexes (**Fe-4** or **Fe-5**/ Ph_2I^+ /NVC, 0.2%/2%/3% w/w). The same complexes were also active toward the ROP of EPOX, with performances dramatically enhanced compared to BAPO (42% versus 18% conversion) in three-component systems and under 385 and 405 nm irradiations.^[49] Similar results were obtained using tripodal Fe(II) Schiff base complexes such as **Fe-6**, and conversions over 30% were achieved both for FRP of TMPTA (after 400 s) and ROP of EPOX (after 800 s) with irradiation centered at 405 nm and **Fe-6**/ Ph_2I^+ /NVC, 0.2%/2%/3% w/w. Besides Schiff bases, polypyridine Fe(II) complexes such as **Fe-7** can be used as PIs for FRP of TMPTA using LEDs at 385 and 405 nm and in three-component systems. However, in this case, the conversions detected were between 20 and 25%. EPOX conversions of $\approx 40\%$



Scheme 9. Selected group VIII metal complexes applied in photopolymerizations.

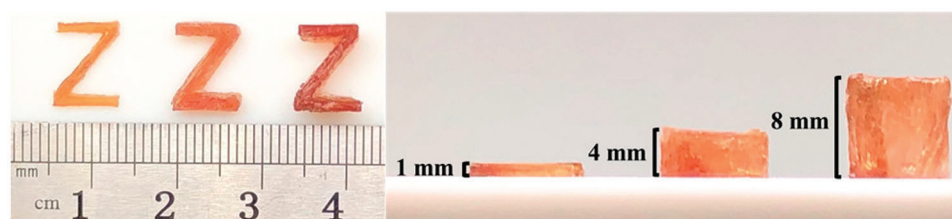


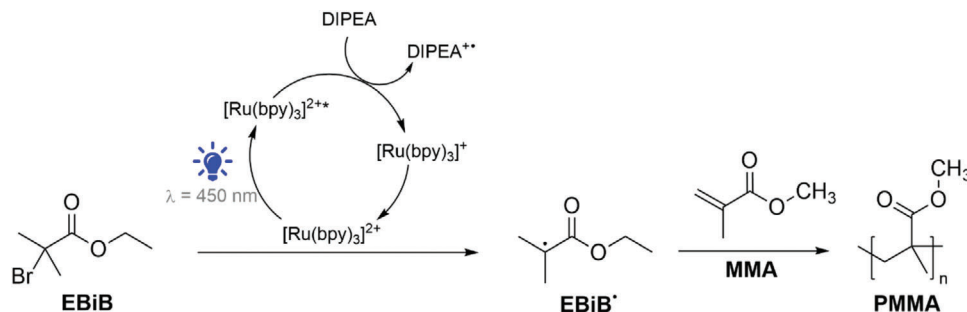
Figure 5. 3D printing objects of different thicknesses obtained by SLA under NIR irradiation, at 25 °C and $[DDE]_0:[CTA]_0:[Ph_2IPF_6]_0:[Fe-2]_0 = 100:1:0.2:0.1$ (see Table 1 for the full names of the mentioned abbreviations). Adapted with permission.^[48] Copyright 2021, American Chemical Society.

were observed after 800 s irradiation at 405 nm. In contrast, due to its relatively low intensity, the photocatalytic performances decreased using the LED@385 nm.^[50]

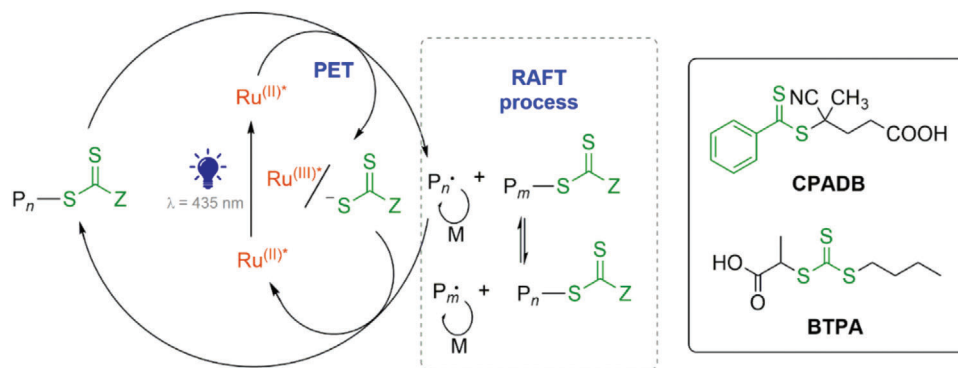
One of the major disadvantages of Fe(II) derivatives is that their photoluminescent lifetimes are extremely short, often in the nanoseconds range. In contrast, photoactive Ru(II) complexes can be considered suitable candidates to be used in photoinitiating systems for their visible-light absorption properties, redox potentials, and long-lived triplet excited states.^[9c,12,51] The “on-off” FRP can be activated or deactivated using visible light since it is strictly dependent on the formation of Ru(II)* species that generate the propagating radicals.^[5b,8c,52] The possible use of $[Ru(bpy)_3]^{2+}$ (**Ru-1**) as PS for the photopolymerization of acrylamide (AM) was observed back in the mid-Eighties in the presence of triethylamine (TEA) as an electron donor.^[53] In recent years, Guo et al. reported a similar system employed for the photopolymerization of MA in the presence of diethyl bromomalonate (DEBrM) as PI and TEA.^[54] The same complex successfully induced ATRP with Xe arc and household lamps in the 420–645 nm range and combined with N,N-diisopropylethylamine (DIPEA). Ethyl α -bromoisobutyrate (EBiB) and benzyl bromide (BB) were used as radical initiators for MMA and higher methacrylates. As illustrated in **Scheme 10**, the sacrificial electron donor DIPEA reduces **Ru-1*** to $[Ru(bpy)_3]^+$, which then reacts with EBiB to form the corresponding radical and initiates the polymerization.^[55]

The photopolymerization of MMA and other methacrylates can also be carried out in heterogeneous conditions by immobilizing **Ru-1** in Nafion-coated silica using EBiB, DIPEA, and household fluorescent lamps as light sources. The system exhibited in all the cases yields above 70% and could be recycled up to five times without significant loss of performance, increasing the overall sustainability of the reaction.^[56]

The same **Ru-1** complex revealed to be also active toward photoinduced electron transfer reversible addition-fragmentation chain transfer polymerization (PET-RAFT). Similarly to what was previously described for **Fe-2**, this type of polymerization requires thiocarbonylthio compounds as PIs and CTAs. Thus, the reaction could be performed with various monomers and in the presence of oxygen, even if radicals are involved in the mechanism. Once excited with proper light irradiation, **Ru-1*** can form $P_n\bullet$ radicals by reducing thiocarbonylthio compounds by PET, as depicted in **Scheme 11**. Then $P\bullet$ can either be deactivated by the Ru(III) species formed via oxidative quenching or participate in the RAFT process. Among the advantages, PET-RAFT can be performed in mild conditions (room temperature and blue light irradiation at 435 nm) and with catalytic loadings in the ppm range, making it extremely appealing to industry. Besides working in organic solvents, **Ru-1** was revealed to be able to induce PET-RAFT also in water affording 95% of *N,N*'-dimethylacrylamide (DMA) conversion after 4 h of irradiation and in the presence of 2-(*n*-butyltrithiocarbonate)propionic acid (BTPA). Good agree-



Scheme 10. Polymerization mechanism for MMA with Ru-1, DIPEA, and EBiB as photoinitiating system (see Table 1 for the full names of the mentioned abbreviations).



Scheme 11. Proposed mechanism Ru-1 catalyzed PET-RAFT (see Table 1 for the full names of the mentioned abbreviations).

ment between theoretical and experimental molecular weights and a symmetrical and narrow distribution were obtained. The possibility of working in water-based solutions allowed exploiting this approach in biological media to prepare protein-polymer bioconjugates.^[57]

One of the potential applications of 3D printing is related to medical devices and bio-inks for the preparation of biocompatible tissues.^[4a] A photoinitiating system based on Ru-1 and sodium persulfate (SPS) was exploited in combination with GelMA (Gelatin-methacryol) and collagen (0.6% wt) for the synthesis of hydrogels under visible light irradiation. Considering also the ability of oxygen inhibition, the best performances were achieved using 1/10 mM/mM Ru-1/SPS.^[58] Following these results, a similar system was applied for the formulation of PEGDA Printlets (3D printed tablets) under the exposure of a smartphone screen (120 s, white background, 100% brightness).^[59] Ru-1 was also tested as PS for a portable DLP 3D printing system enabled by the camera light of a smartphone. The polymeric structures prepared using 40% v/v of commercially available PEGDA together with $2 \cdot 10^{-3}$ M/20 $\cdot 10^{-3}$ M Ru-1/SPS are shown in Figure 6 (operating speed: $96 \mu\text{m s}^{-1}$). Due to its visible light absorption ($\lambda_{\text{max}} = 508 \text{ nm}$), Ponceau 4R (2.5% w/w) was exploited as a photoabsorber to limit the depth of light penetration and thus ink over-curing, allowing the preparation of structure even with intricate internal geometries.^[60]

Besides, in FRP, Ru-1 was efficiently used as PS to polymerize EPOX and limonene dioxide (LDO) under green light irradiation in the presence of TTMSS and Ph_2I^+ . As previously observed, no photopolymerization was detected without TTMSS, and its use is

crucial to obtain conversions over 60% as the initiation process is governed by the presence of strong oxidant Ru(II)* species and silylium TTMSS⁺ cations. After four minutes, conversions over 95% and 60% of EPOX were obtained under air with a laser diode centered at 457 and 532 nm. Using the same experimental conditions, the conversions were only $\approx 60\%$ for LDO at 457 nm.^[38,39,61] Since the formation of radical Ph• and TTMSS• by hydrogen abstraction is required to form TTMSS⁺, the three-component systems are also active toward FRP.^[39,62] Despite the better absorption properties in the 350–600 nm range of $[\text{Ru}(\text{phen})_3]^{2+}$ (phen = 1,10-phenanthroline, Ru-2), the three-component system with TTMSS and Ph_2I^+ exhibited lower efficiencies, and conversions $\approx 45\text{--}48\%$ of EPOX were achieved after 180 s of irradiation with white and blue light LEDs. The lower efficiency can be attributed to the higher oxidation potential of Ru-2 compared to Ru-1, which determined lower reactivity toward the iodonium salt.^[38,61,63]

Since Ru-1 and Ru-2 were active toward FRP and ROP under green light, testing them in a hybrid system composed of 50%/50% w/w of TMPTA and EPOX was possible. After less than four minutes, conversions of 65% for Ru-1 and 45% for Ru-2 were achieved under air and with incandescent bulb irradiation.^[39,61]

Besides the homoleptic complexes, the heteroleptic cyclometallated complexes Ru-3 and Ru-4 containing 2-phenylpyridine (ppy), phen, or bpy as chelating ligands, and two coordinated acetonitrile molecules were active toward the photopolymerization of MMA, St and *n*-butyl acrylate (*n*BA) affording conversions $\approx 70\%$ under visible light irradiation and in the presence of EBiB as PI. In contrast to St, the polymerization of *n*BA at room

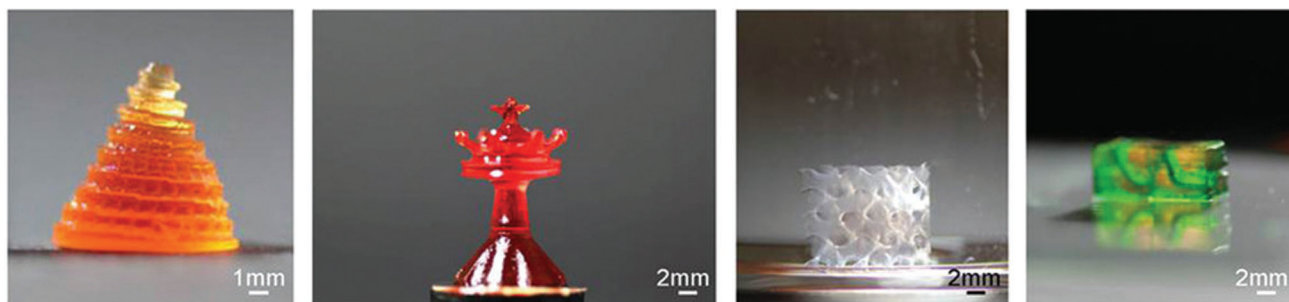
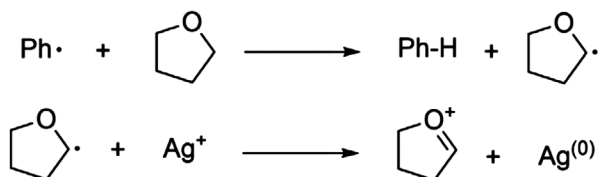


Figure 6. Structures obtained with a smartphone-enabled 3D printer (40% v/v PEGDA, $2 \cdot 10^{-3}$ M/ $20 \cdot 10^{-3}$ M Ru-1/SPS, 2.5% w/w Ponceau 4R). Adapted with permission.^[60] Copyright 2021, American Chemical Society.



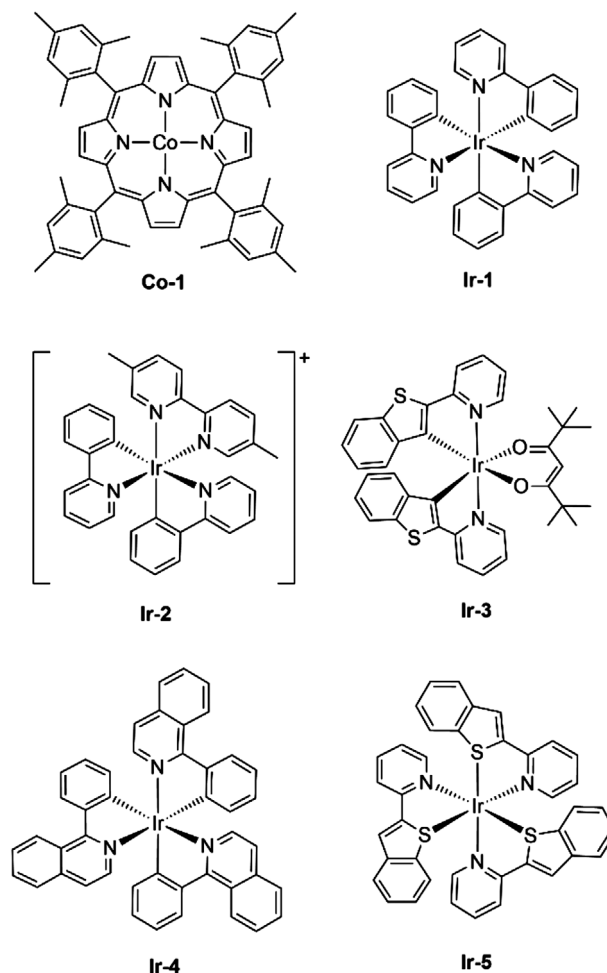
Scheme 12. Proposed mechanism for the ROP of IDE catalyzed by Ru-5/AgSbF₆/THF.

temperature afforded 90% of conversion after 8 h of irradiation. The high efficiency in the photoinduced homopolymerization of the three different monomers was applied for the synthesis of block copolymers of MMA and nBA with St.^[64]

The only example of a Ru(II) complex with P-donor ligands tested for photopolymerization is [RuCl₂(PPh₃)₃] (**Ru-5**). The derivative afforded complete conversion of PEGDA after 50 s of irradiation with a Xe-Hg lamp, owing to the homolytic cleavage of the P-Ph bond upon UV light irradiation. Although the complex was tested in laminate, the FRP starts after an induction period because the radical R• reacts with the remaining O₂, and the process begins only when all the oxygen is consumed. The same complex tested for the ROP of diepoxide (isosorbide diglycidyl ether, IDE) required 3% wt of AgSbF₆ and 1 mL of THF to achieve conversions ≈50%. As highlighted in **Scheme 12**, silver nanoparticles are obtained as suggested by the brown color of the final product, and THF is essential for the reaction to proceed since it generates the initiating cationic species.^[65]

4.5. Group IX Metal Complexes

Considering group IX metals, Co(II) complexes, such as metalloporphyrins, can catalyze radical polymerization reactions.^[66] However, Co(II) porphyrins can also undergo photocleavage to generate organic radicals and initiate the FRP. Organo-cobalt initiators were prepared by thermal polymerization of **Co-1** (see **Scheme 13**) in the presence of MA and 2,2'-azobisisobutyronitrile. Then, the photopolymerization of N,N-dimethylacrylamide (DMA) was carried out inside a J. Young NMR tube. In the absence of light, the conversion was only ≈8% after 12 h; while using a 500 W Xe lamp, 98% conversion was detected for the **Co-1**-based initiator without any additive.^[67] The same complex was also active toward FRP of acrylates, such as MA and n BA, under visible light irradiation. The study reported



Scheme 13. Selected group IX metal complexes applied in photopolymerizations.

by Fu et al. highlighted the direct influence of light intensity since values between 3 and 7 mW cm⁻² permitted to better control the photopolymerization of MA in terms of molecular weight distribution and conversions. It is worth mentioning that this aspect is also particularly relevant for applications in 3D printing. Instead, higher light intensities generated an excess of organic radicals by

over-irradiation of Co–C bonds that determined poor control of the photopolymerization process.^[68]

Like Ru(II) complexes, photoactive Ir(III) complexes were efficiently used as PSs being more versatile in terms of the synthesis and tuning of the photochemical properties. Moreover, just like Fe(II) complexes, Ir(III) derivatives are potentially applicable both in oxidative (Ir/iodonium salt/silane) and in reductive (Ir/amine/alkyl halide) mechanisms. *fac*-[Ir(ppy)₃] (ppy = 2-phenylpyridine, **Ir-1**) was first tested by Hawker and coworkers for the photopolymerization of MMA with ethyl α -bromophenylacetate (EBPA) as co-initiator under 50 W fluorescent lamp. The reduction of the photocatalyst from 0.2 mol.% to 0.005 mol.% allowed better control of the polymerization and molecular weight distribution. It is worth noting that, in this case, the system induced the photopolymerization of methacrylic acid (MAA), which is normally challenging due to the presence of the acid functionality.^[69] Following these results, the same group reported the synthesis of block copolymers using acrylic acid and ethyl acrylate, achieving good agreement between experimental and theoretical molecular weights, with an average ratio of acrylic acid from 5 to 20%.^[70] Using a water-soluble monomer, such as poly(ethylene glycol) methacrylate (PEGMA), permitted the recycling of the catalyst by the addition of water, without significant loss in terms of efficiency.^[71] The performances of **Ir-1** as a photocatalyst were better than **Ru-1** due to the longer lifetimes (1.5 μ s vs. 0.45 μ s) and the lower oxidation potential (0.77 V vs. 1.3 V).^[38,63,72] In particular, the three-component system **Ir-1**/TTMSS/Ph₂I⁺ (0.2%/3%/2% w/w/w) afforded 60% conversion of EPOX after 120 s of Xe lamp irradiation under air, while to obtain the same conversion **Ru-1** needed 180 s. Owing to the advantages listed before and the enhanced performances compared to Ru(II) species, a wide variety of Ir(III) derivatives was synthesized and tested in photoinitiating systems.^[38,73] Like group VIII elements, **Ir-1** was active toward PET-RAFT processes, and the polymerization of MMA using 1 ppm of complex and CPADB as PI and CTA afforded 73% of monomer conversion after 67 h of blue LED irradiation. To further investigate the potentiality of this system, Boyler and coworkers synthesized multiblock copolymers by multiple chain extensions under air, obtaining the product in high purity and without any supplementary addition of photocatalyst.^[74] The same authors extended the use of the system for the PET-RAFT of non-conjugated monomers like NVC using xanthate or dithiocarbamate as CTA. The polymerization rates were not affected by the presence of air, affording the polymers in good yields and with narrow molecular weight distributions. The oxygen tolerance was attributed to the reducing properties of **Ir-1** that could easily convert O₂ into inactive superoxide species.^[75]

Instead, when **Ir-2** was used in combination with phenacyl bromide (PABr) and *N*-methyl-*N,N*-diethanolamine (MDEA), conversions over 70% for pentaerythritol tetraacrylate (PETA) were achieved in laminate after 180 s of Xe lamp irradiation (**Ir-2**/MDEA/PABr, 0.2%/4.5%/3% w/w). The conversion dropped to 35% under the same experimental conditions when the photopolymerization was conducted under air. This system was more efficient than the one obtained using **Ru-1** and comparable to metal-free dyes such as Eosin Y (**OC-8** in Scheme 1) or titanocene derivatives.^[76] When the same **Ir-2** complex was applied for ROP with TTMSS and Ph₂I⁺ (0.2%/3%/2% w/w/w), the conversion

of EPOX was \approx 60% after 180 s of blue LED irradiation. Since the Ir(III) photocatalyst is regenerated in the photoinitiating system and incorporated in the final product at its initial oxidation state, the polymer exhibited photoluminescent properties that could be tuned from 480 to 620 nm by acting on the coordinated ligands.^[73a]

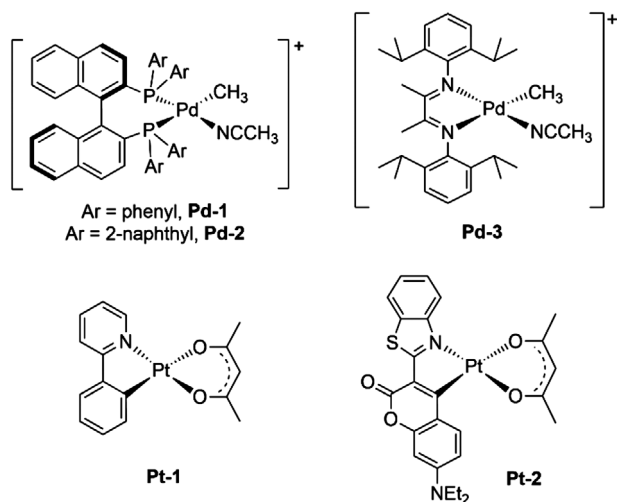
The heteroleptic **Ir-3** complex exhibited improved photoluminescent properties in comparison to **Ir-1**, being characterized by a bathochromic shift of the absorption maximum from 372 nm (**Ir-1**) to 476 nm (**Ir-3**) and almost a 3.5 times longer luminescent lifetime (1300 ns for **Ir-1** vs. 4400 ns for **Ir-3**). The derivatives exhibited good photocatalytic activity toward radical and cationic photopolymerization under mild conditions (blue-green light between 457 and 532 nm). Conversions of EPOX above 50% were achieved under air after 400 s in a two-component system with Ph₂I⁺ (1%/2% w/w) using laser diode irradiation centered at 457 nm or a halogen lamp. Instead, when a laser diode centered at 532 nm was employed, similar conversions could be obtained only in a three-component system with NVC (1%/2%/3% w/w). FRP of TMPTA was conducted in laminate at 457 nm affording final conversions of \approx 30% for **Ir-3**/PABr (0.5%/3% w/w) and 47% for **Ir-3**/PABr/MDEA (0.5%/3%/5% w/w). Besides being active in reductive cycles, **Ir-3** was the first example of a complex working in an oxidative cycle inside the photoinitiating system. Like **Ir-1**, **Ir-3** required low catalytic loading to efficiently control the polymerization as its role was only to induce the formation of active species without terminating the propagating chain. Under the same experimental conditions, **Ir-1** was inefficient due to the lower molar extinction coefficient at this wavelength. Like **Ir-2**, **Ir-3** was not degraded during the photopolymerization and was embedded in the final product, thus conferring photoluminescent properties to the polymer.^[77]

However, one of the major drawbacks of Ir(III) complexes, affecting the overall conversion of the monomers, is related to their low solubility in the reaction media. For instance, under the same experimental conditions, [Ir(piq)₃] (**Ir-4**) and [Ir(btpy)₃] (btpy = 2-(benzothiophen-2-yl)pyridinato, **Ir-5**) were tested for the hybrid photopolymerization of 50%/50% w/w EPOX/NVC with a LED@462 nm in the three-component system with TTMSS and Ph₂I⁺ (0.2%/3%/2% w/w). After 400 s, 85% conversion was detected for **Ir-4**, while it was much lower (\approx 40%) for **Ir-5** because of its lower solubility in the monomer.^[38,78]

4.6. Group X Metal Complexes

Only noble metal complexes were tested for photopolymerization reactions between group X elements. Pd(II) complexes were deeply investigated as catalysts for the polymerization of olefins.^[79] Nevertheless, Pd(II) derivatives proved to be efficient candidates to be applied in photoinitiating systems for photo-ATRP.^[80] In 2016, Son and Inagaki reported aryl-substituted BINAP-Pd(II) complexes (**Pd-1** and **Pd-2** in Scheme 14, 1 mol.%) that were exploited for the photopolymerization of 4-methoxystyrene (4-OMe-St) under UV light.^[81]

Under the same experimental conditions, the naphthyl-substituted **Pd-2** exhibited enhanced catalytic performance compared to **Pd-1**, with yields \approx 60% and 20% after 10 h. The photopolymerization could be stopped and resumed by switching off



Scheme 14. Selected group X metal complexes applied in photopolymerizations.

and on the light source, without any significant molecular weight or distribution difference from the polymer obtained by continuous irradiation. In this case, the photopolymerization is facilitated by the light-mediated insertion of 4-OMe-St, accelerating the overall reaction, as highlighted in **Scheme 15**.^[81]

The copolymerization of MA with α -olefins is normally challenging because of the low degree of acrylate effectively incorporated into the final product. In this sense, using light in combination with the cationic diimine Pd(II) complex **Pd-3** was beneficial to overcome this problem. **Pd-3** induced the polymerization of MA under blue-light irradiation centered at 460 nm, while hexene required dark conditions to achieve full conversions. The possibility of switching the catalytic activity from insertion to radical mechanism with light is known as metal-organic insertion/light-initiated radical polymerization. Owing to its “on-off” nature, it was possible to obtain diblock copolymers by subsequent selective polymerization of hexene in the dark and MA at 460 nm.^[82]

Due to their millisecond-long lifetimes and good absorptions in the visible spectra, another class of derivatives that can be employed in photoinitiating systems is represented by the cyclometallated Pt(II) complexes **Pt-1** and **Pt-2**.^[38] Both complexes were active toward the ROP of EPOX in a three-component system together with TTMSS and Ph_2I^+ (0.2%/3%/2% w/w). Owing to the better absorption properties of **Pt-2** in the 400–540 nm range, conversions above 70% were obtained after 1000 s of halogen lamp irradiation. Instead, using **Pt-1** or an organic system based on 7-diethylamino-4-methyl coumarin (**OC-2** in Scheme 1), the conversion decreased dramatically to 59% and 20%, respectively. As previously observed, no conversion was detected using the corresponding two-component system with Ph_2I^+ due to the rapid photodegradation of the complex, which was instead regenerated by the silyl radical in three-component systems. This process was confirmed by flash laser photolysis experiments and photoluminescence spectra of the final polymer. Owing to the ability of **Pt-2**/TTMSS/ Ph_2I^+ (0.2%/3%/2% w/w) to generate both radicals and cations, the system was tested toward the hybrid polymerization of TMPTA and EPOX (50%/50% w/w). Final conversions of 60% for TMPTA and 50% for EPOX were detected after 1000 s

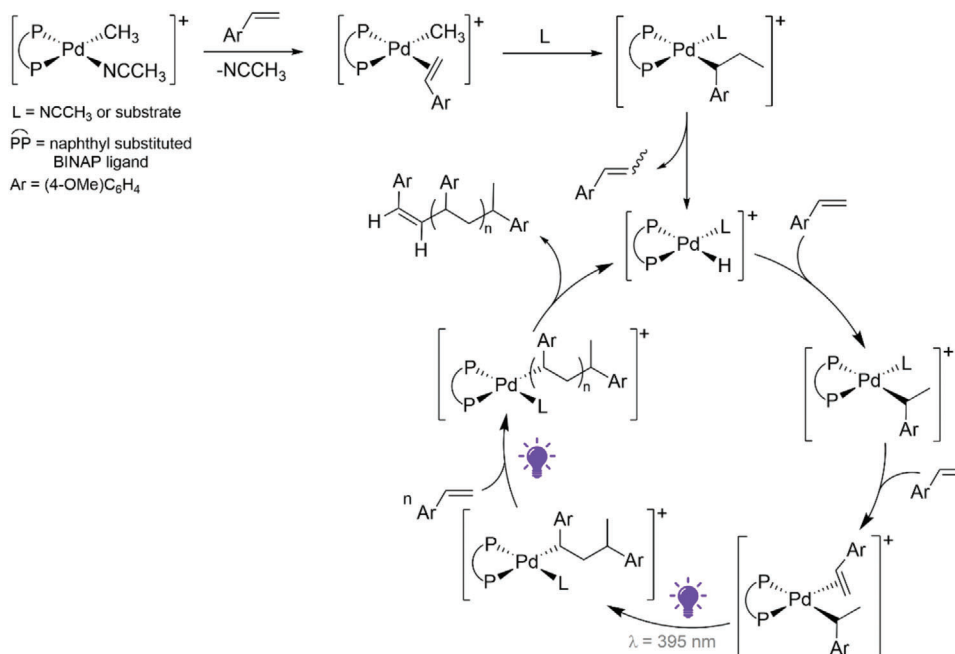
of halogen lamp irradiation. However, **Pt-1** and **Pt-2** were active only in an oxidative environment, and no catalytic activity was observed in the presence of amines and alkyl halides.^[83] Despite the impressive performances in photoinitiating systems, the high costs of Pt and the long irradiation times required prevent any possible application in industry, and no further study on analogous compounds was reported.

4.7. Group XI Metal Complexes

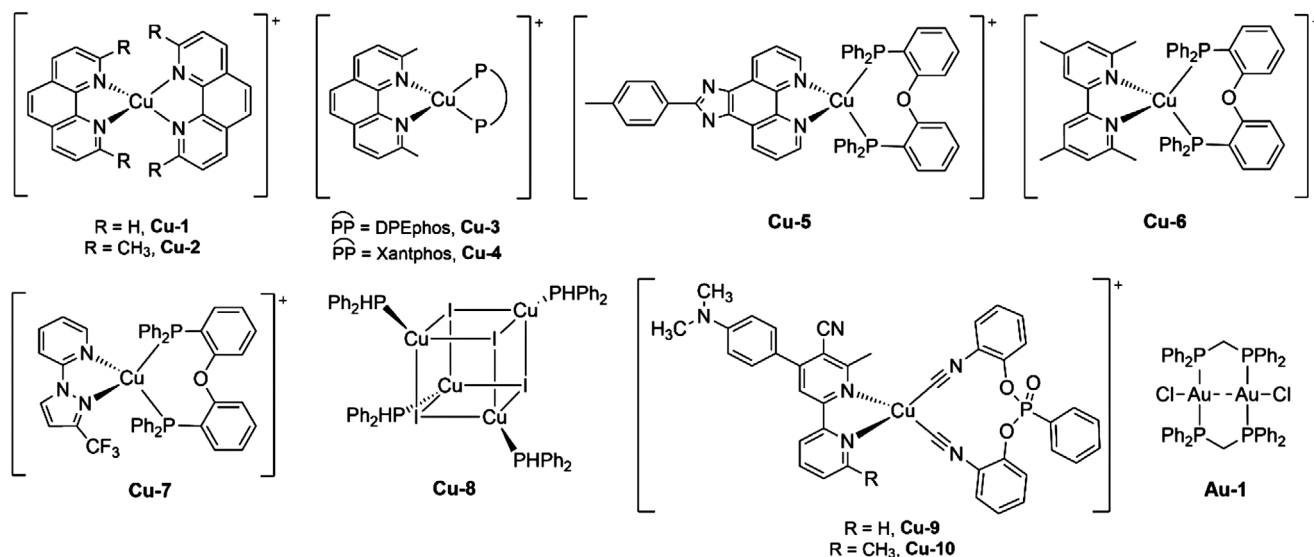
As regards coinage metals, only copper, and gold complexes were applied in photopolymerization reactions. It should be mentioned that using Cu(II) salts to generate in situ Cu(I) species in the presence of light and a reducing agent is a commonly used approach to perform photoinduced controlled radical polymerization of acrylates.^[17a,84] Instead, concerning luminescent Cu(I) complexes, growing attention has been devoted to their use in photoinitiating systems owing to the moderate cost, low toxicity, and high availability of this metal center. The possibility of tuning photophysical properties (such as absorption and emission maxima) by acting on the coordinated ligands represents another important advantage, making Cu(I) extremely versatile.^[38,85]

The photophysical properties of Cu(I) complexes containing phenanthroline and its derivatives as N-donor ligands have been known since the Eighties.^[86] However, the application of Cu(I) complexes in photoinitiating systems was first described in 2014 by Lalevéé et al. when $[\text{Cu}(\text{phen})_2]\text{BF}_4$ (**Cu-1**, see **Scheme 16**) was efficiently used for the photo-ATRP of MMA under blue LED irradiation centered at 465 nm and in the presence of EBPA as co-initiator. TEA was added to reduce oxidative quenching, thus regenerating the activator and increasing the polymerization rates. In this case, conversions were still quite low, with values of 28% after 82 h of irradiation.^[87] The same authors later increased the overall conversion to 38% using $[\text{Cu}(\text{dmp})_2]\text{BF}_4$ (**Cu-2**, dmp = 2,9-dimethyl-1,10-phenanthroline) in a three-component system composed by Ph_2I^+ and NVC (0.2%/2%/3% w/w) for the photopolymerization of TMPTA at 457 nm.^[6]

Regarding heteroleptic complexes, $[\text{Cu}(\text{dmp})(\text{DPEphos})]\text{BF}_4$ (**Cu-3**, DPEphos = bis(2-diphenylphosphino)phenyl ether) and $[\text{Cu}(\text{dmp})(\text{Xantphos})]\text{BF}_4$ (**Cu-4**, Xantphos = 4,5-bis(diphenylphosphino)-9,9-dimethylxanthene) bearing 2,9-dimethyl-1,10-phenanthroline (dmp) as chelating N-donor ligand were tested for the photopolymerization of TMPTA.^[6,38] The three-component photoinitiating system obtained using **Cu-3**, Ph_2I^+ , and NVC (0.2%/2%/3% w/w) afforded conversions $\approx 60\%$ in laminate both using halogen lamp and LED irradiations centered at 405 and 455 nm. The system worked under air with lower photopolymerization rates and conversions of $\approx 13\%$ due to oxygen inhibition. The three-component system exhibited better performances as a photoinitiating system than the commonly used bisacylphosphine oxide (BAPO, **OC-1** in Scheme 1) that under the same experimental conditions (LED@405 nm, laminate, 0.2% wt) afforded 53% of conversions of TMPTA. Instead, **Cu-4** determined lower monomer conversion (18% at 405 nm and 26% at 457 nm) due to its small molar extinction coefficient at the considered wavelengths. The same three-component systems containing **Cu-3** and **Cu-4** were also active toward the ROP of EPOX. Conversions over 60% after 800 s



Scheme 15. Proposed mechanism for Pd-2-catalyzed polymerization of 4-OMe-St under UV light irradiation.



Scheme 16. Selected group X metal complexes applied in photopolymerizations.

were achieved for the system **Cu-3**/Iod1/NVC (0.2%/2%/3% w/w) under air and halogen lamp irradiation. The photocatalytic performances dropped to 32% of the conversion of EPOX once a laser diode ($\lambda = 405 \text{ nm}$) was used as the light source. Instead, when Ph_2I^+ was exploited as PI instead of Iod1, conversions were $\approx 60\%$ working with LED irradiations centered at 405 and 455 nm. Owing to its photocatalytic ability both toward FRP and ROP, **Cu-3**/ Ph_2I^+ /NVC (0.2%/2%/3% w/w) was able to induce the formation of interpenetrated polymer networks (IPNs) using a mixture of TMPTA and EPOX (50%/50% w/w) as monomers, and upon halogen lamp irradiation. Since oxygen

slows down FRP, different results were obtained performing the photopolymerization in laminate or under air. In the former, higher conversions of TMPTA were detected compared to EPOX (74% versus 38%), while in the latter, it was the opposite (30% of TMPTA versus 45% of EPOX). The conversion of TMPTA is 2.5 times higher in laminate than under air because FRP is faster than ROP, so the generated radicals are consumed to initiate the first process.^[88] The same complex **Cu-3** was applied to the photopolymerization of low viscosity acrylates using Iod as co-initiator and Sn(II) bis(2-ethylhexanoate) or Bi(III) tris(2-ethylhexanoate) as reducing agents. The reaction proceeded with

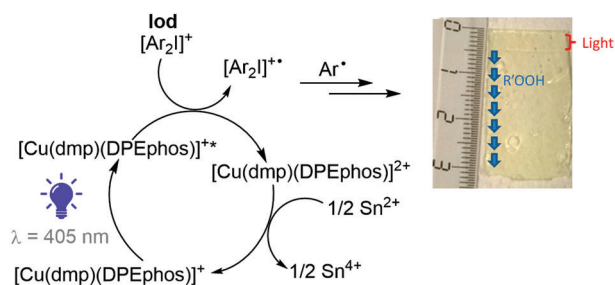


Figure 7. Proposed mechanism for the photopolymerization of methacrylates in the presence of **Cu-3**, Iod ($Ar = 4\text{-tert-butylphenyl}$), and Sn(II) bis(2-ethylhexanoate) and picture of the polymer obtained from irradiated to shadowed areas. Adapted with permission.^[89] Copyright 2017, American Chemical Society.

low irradiance LEDs ($I = 2.5 \text{ mW cm}^{-2}$) or solar irradiation ($I < 6.0 \text{ mW cm}^{-2}$) and low Cu(I) loading (0.1–0.3% wt). 55% and 65% of conversions were achieved after 150 s of LED exposure and 90 s of solar light irradiation for 1.4 mm thick samples. The reaction between Cu(I) and ROOH determined the formation of active RO• species, while with Cu(II), the same process generated RO₂• radicals that were instead less reactive. The addition of Sn(II) or Bi(III) compounds as reducing agents helps to lower the concentration of Cu(II) and the quantity of required photocatalyst, as observable in **Figure 7**. The soft irradiation generated RO₂• species that converted into hydroperoxides (ROOH) by hydrogen abstraction and diffused from irradiated to shadowed areas, thus allowing the photopolymerization to continue in the absence of light by reduction of Cu(II) to Cu(I) and the generation of new reactive RO• species.^[89]

Besides **Cu-3** and **Cu-4**, an expansive library of Cu(I) derivatives was reported by Lalevé and coworkers using bpy and other phen derivatives as N-donors. **Cu-5** exhibited enhanced photocatalytic performances owing to the higher molar extinction coefficient, particularly at 457 nm. In a two-component system with Ph₂I⁺ (0.2%/2% w/w), 36% conversion of TMPTA was detected after 500 s of laser diode irradiation at 405 nm. Instead, when a halogen lamp or a laser diode centered at 457 nm were used as light sources, the conversions increased to 50%. Adding NVC (3% wt) boosted conversions to 59% and 57%, respectively, with a blue laser ($\lambda = 457 \text{ nm}$) and halogen lamp irradiation. Apart from working in an oxidative mode, **Cu-5** displayed excellent photocatalytic ability also in the presence of MDEA and PABr with conversions of TMPTA equal to 59% (LED@405 nm), 55% (LED@455 nm), and 49% (halogen lamp) after 400 s of irradiation. The system **Cu-5**/Ph₂I⁺ was also active toward the thiol-ene photopolymerization with a trimethylolpropane tris(3-mercaptopropionate) (TPTM)/(DVE-3) blend (57%/43% w/w). After 200 s of laser diode irradiation at 457 nm, 85% and 57% of conversions were respectively measured for the vinyl ether and the thiol functions.^[6,85,90]

A similar ligand, based on the bpy fragment, proved that using Cu(I) complexes exhibiting thermally activated delayed fluorescence (TADF) can also benefit photopolymerization reactions.^[91] Normally these properties are exploited for OLEDs (organic light-emitting diodes) as they can potentially reach 100% of internal quantum efficiency owing to the possibility of harvesting both singlet and triplet excitons.^[92] The heteroleptic **Cu-6** complex

sketched in Scheme 16 was tested with Iod (0.5%/1% w/w) toward the FRP of BisGMA/TEGDMA blends with LED irradiation centered at 405 nm, determining 60% of conversion after 400 s. Under the same experimental conditions, the corresponding two-component system with a non-TADF Cu(I) complex bearing 4,4'-dimethyl-2,2'-dipyridine as chelating N-donor afforded only 30% of conversion. Similar results were also obtained for the ROP of EPOX in three-component systems with NVC as an additive (0.5%/1%/1% w/w). Since the extinction coefficients of the two Cu(I) complexes are similar, the different outcomes were ascribed to the photoluminescent lifetimes that were 100 times longer for **Cu-6** if compared to the non-TADF derivative (2.5 μs vs. 0.02 μs). The prolonged lifetime at the excited state determined a better interaction with the co-initiator and the additive, thus enhancing the overall photopolymerization performances.^[91]

In addition to bpy and phen derivatives, pyridine-pyrazole ligands were applied as chelating N-donors to prepare homo- and heteroleptic Cu(I) complexes tested for the FRP of acrylates and ROP of EPOX with LED irradiation at 405 nm. The best performances for the former were observed for two-component systems based on **Cu-7** (see Scheme 16) and Ph₂I⁺ (0.5%/1% w/w), with conversions $\approx 65\%$ after 100 s of exposure. When Iod was applied as an additive, the corresponding two-component system with **Cu-7** (0.5%/1% w/w) was able to initiate the FRP of a bisphenol A-glycidyl methacrylate (BisGMA)/triethylene glycol dimethacrylate (TEGDMA) blend (70%/30% w/w) both in laminate (25 μm thick sample) and under air (1.4 mm thick sample). Conversions $\approx 47\%$ and 69% were measured after 100 s irradiation with LED@405 nm. Adding EDB (1% wt) as a hydrogen donor increased the conversion up to 80%. The good performances of this three-component system were then tested for 3D printing using a LED projector at 405 nm.^[93] It is important to underline that the previously mentioned two-component system consisting of **Cu-7**/Iod (0.5%/1% w/w) exhibited the best performances in terms of polymerization rates and efficiency for the ROP of EPOX. Indeed, conversions of EPOX $\approx 48\%$ were detected after 400 s of LED irradiation centered at 405 nm. Differently from the previously described examples, 1% wt of 9H-carbazole-9-ethanol (CARET) was used as an additive instead of NVC, increasing the conversion to 63%. This enhancement was attributed to the regeneration of the complex by CARET, avoiding the consumption of the PI during the process.^[6,93]

Another class of complexes, used as co-initiators in the presence of Norrish Type II PIs isopropylthioxanthone (ITX) or camphorquinone (CQ) for the FRP of TMPTA, are cubane derivatives having the general formula [Cu(μ -1)(phosphine)]₄. Triphenylphosphine and PPh₂ were used as P-donor ligands, but no efficient polymerization was observed with the former due to the absence of labile hydrogens. Instead, the two-component systems based on ITX/**Cu-8** and CQ/**Cu-8** (1%/1% w/w) exhibited comparable performances to the commonly used ITX/EDB and CQ/EDB both under air (1.4 mm thick sample) and in laminate (25 μm thick sample), proving to be a valid and environmentally friendly alternative to aromatic amines (see **Figure 8**). The system ITX/**Cu-8** was also tested for preparing 3D printing resins starting from TMPTA. The final polymer was obtained with high spatial resolution and a writing time of under one minute. Since **Cu-8** was linked through the P–H bond, the final polymer was

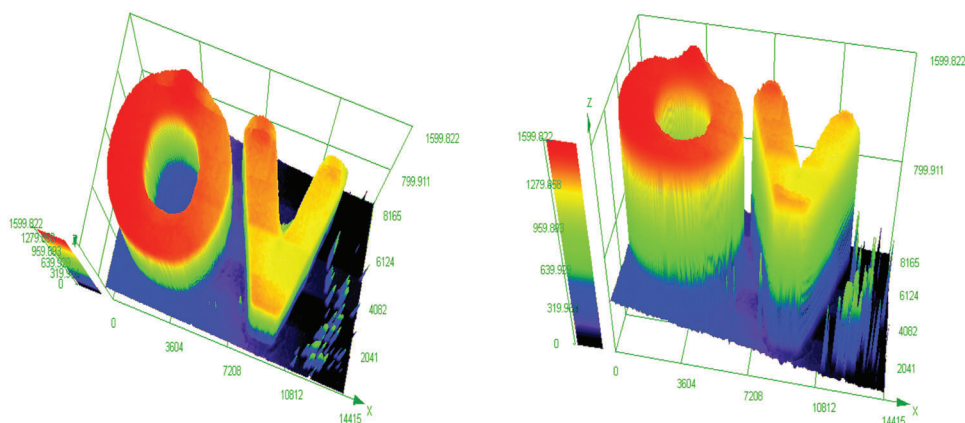


Figure 8. 3D printing experiments using ITX/Cu-8 (1%/1% w/w) in TMPTA (laser diode centered at 405 nm, thickness = 1599 μm ; the full names for the mentioned abbreviations are collected in Table 1). Reproduced with permission.^[94] Copyright 2021, Royal Society of Chemistry.

characterized by luminescent properties strictly comparable to those of the free complex.^[94]

Similar 3D patterns were recently obtained using heteroleptic Cu(I) complexes having a C-donor ligand, i.e. bis(2-isocyanophenyl)phenylphosphonate instead of phosphines in combination with bpy derivatives (see complexes **Cu-9** and **Cu-10** in Scheme 16). The 3D experiments were carried out using TA or TMPTA as monomers, a laser diode at 405 and 455 nm, and three-component systems containing Iod and/or N-phenyl glycine (NPG) as co-initiators and N,N -dimethyl-p-toluidine (DMPT) as additive. In 1.4 mm thick samples, the system **Cu-9**/Iod/NPG and **Cu-10**/Iod/NPG (0.1%/1%/1% w/w) afforded monomer conversion over 80% both at 405 and 455 nm. When DMPT was introduced as an additive, the systems allowed the preparation of high-spatial-resolution 3D patterns by direct laser writing (DLW) in two to three minutes (thickness of $\approx 2500 \mu\text{m}$). Despite the similarities of the ligand with BAPO, the potential role of the bis(2-isocyanophenyl) phenylphosphonate as organic PI was not investigated separately. Similar to **Cu-3** (see Figure 7), the initiation of the photopolymerization was attributed to the formation of $\text{Ar}\bullet$ ($\text{Ar} = 4\text{-tert-butylphenyl}$) radicals from Iod by reaction with the Cu(I) complexes at the excited state.^[95]

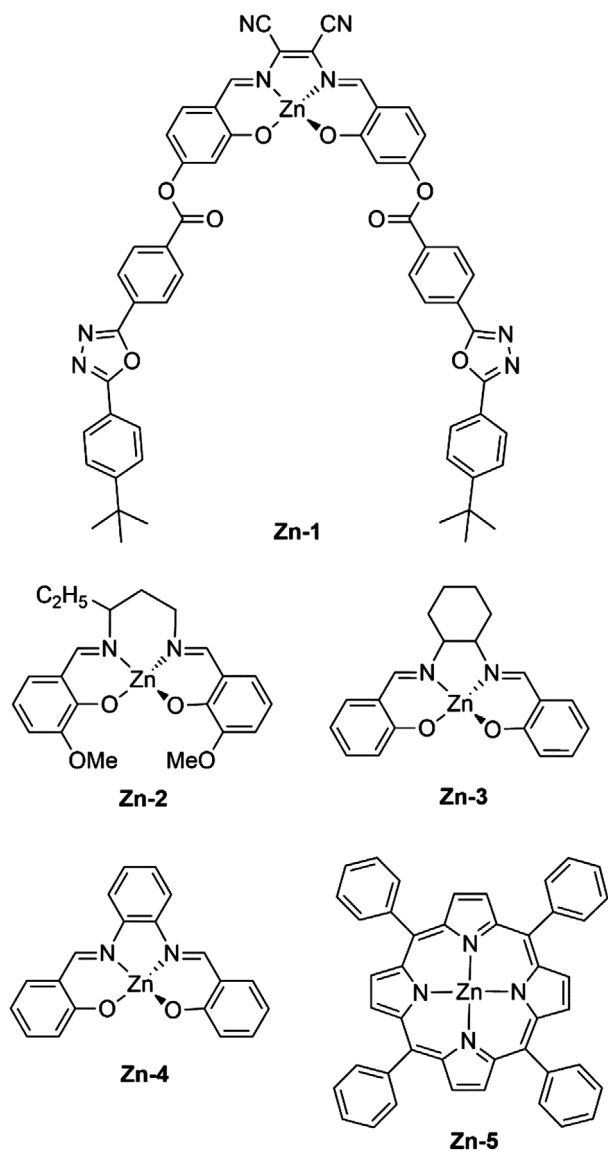
Finally, only one example could be found for what concerns gold complexes. Herein, radical photopolymerization was initiated by low loadings (1.25 mol.% vs. co-initiator) of the binuclear Au(I) complex $[\text{Au}_2(\mu\text{-dppm})_2]\text{Cl}_2$ (dppm = di(phenylphosphino)methane, **Au-1**) using EBPA as co-initiator and MMA as a monomer in solution. Conversions of 75% were obtained in CH_2Cl_2 and using UV light irradiation at 350 nm. In laminate, the two-component system exhibited a faster polymerization rate for TMPTA than EBPA/**Ir-1**. Conversions of 38% were achieved after 400 s of irradiation with blue light at 405 nm, while for the same system with **Ir-1**, it was 33% after 800 s.^[96]

4.8. Group XII Metal Complexes

Group XII metals are not properly considered transition metals but are normally called “post-transitional” due to their completely filled *d*-shell. The investigation in photoinitiating systems

is limited to Zn(II) derivatives, probably because of the extreme toxicity of cadmium and mercury. The luminescence of Zn(II) derivatives can be normally assigned to the fluorescence of ligands, enhanced by coordination to the metal center, and therefore characterized by nanosecond-long lifetimes.^[38] In 2013, Lalevée and coworkers tested the Zn(II) complexes **Zn-1** to **Zn-3** (see Scheme 17) in multicomponent systems for FRP of TMPTA as well as for cationic polymerization of tri(ethylene glycol) divinyl ether (DVE-3).^[97] The complexes mentioned above absorb intensively in the visible spectrum; in particular, **Zn-1** presents the highest molar extinction coefficient equal to $38000 \text{ M}^{-1}\text{cm}^{-1}$ at 550 nm. The combination of **Zn-1**/TTMSS/ Ph_2I^+ (0.2%/3%/2% w/w) exhibited the best results, with final conversions up to 30% for TMPTA in laminate with several light irradiations (halogen lamp and laser diode centered at 457 and 532 nm). As previously observed for the other systems, the silane additive is necessary to obtain any conversion. The exchange of TTMSS with DVE-3 as an additive resulted in an increased conversion for **Zn-1** up to 45% within two minutes (**Zn-1**/DVE/ Ph_2I^+ , 0.2%/6%/2% w/w). A similar behavior was observed for **Zn-2** and **Zn-3**, although they generally show a slower conversion. It is worth noting that the polymerization efficiency shows a trend following **Zn-1** > **Zn-2** > **Zn-3** due to the different overlap between the absorption properties of the metal complexes and the emission spectrum of the light source used. The system **Zn-1**/TTMSS/ Ph_2I^+ (0.2%/3%/2% w/w) was also tested for the cationic photopolymerization of DVE-3 in laminate and gave a final conversion of 80% after ten minutes using a laser diode source centered at 532 nm. Also, in this case, TTMSS is necessary to obtain any polymerization. Since **Zn-1** was active both toward FRP and cationic polymerization, it was investigated using a blend of TMPTA/DVE-3 (50%/50% w/w) in laminate and under halogen lamp irradiation. Even in two-component systems without TTMSS (**Zn-1**/ Ph_2I^+ or **Zn-1**/Iod1), it was possible to obtain conversions $\approx 80\%$ for both monomers, but its addition remained beneficial for the overall photocatalytic performances.^[97]

The previous examples were all investigated in laminate. Nevertheless, the same group proposed another complex (**Zn-4**) that could act as PI or additive to achieve high conversions of TMPTA via FRP under air. As observable in Figure 9 (curve A), the same process using only the organic PI 2,2-dimethoxy-



Scheme 17. Group XII metal complexes applied in photopolymerizations.

2-phenylacetophenone (DMPA, **OC-4** in Scheme 1) afforded conversions under 15% after 300 s of Hg-Xe lamp irradiation due to oxygen inhibition. Adding **Zn-4** to DMPA (**DMPA/Zn-4**, 1%/0.3% w/w) allowed a final conversion of 30% and faster polymerization rates (see curve B, Figure 8). As previously described for other systems, the formation of $\text{RO}_2\bullet$ species by the scavenging reaction is detrimental to FRP. However, when **Zn-4** is added to DMPA, no peroxy radicals are formed, as confirmed by electron spin resonance/spin trapping experiments, suggesting they are scavenged by the complex forming the initiating species.^[98]

Another class of Zn(II)-based PIs are metalloporphyrins, which can be used as activators for PET-RAFT polymerization. In 2015 Boyer et al. used zinc tetraphenylporphyrin **Zn-5** as an additive, exhibiting a selective activation toward trithiocarbonates. This molecular recognition is unusual, as strong reducing agents are normally needed to start the RAFT process for acrylates. Interestingly, the polymerization rate could be con-

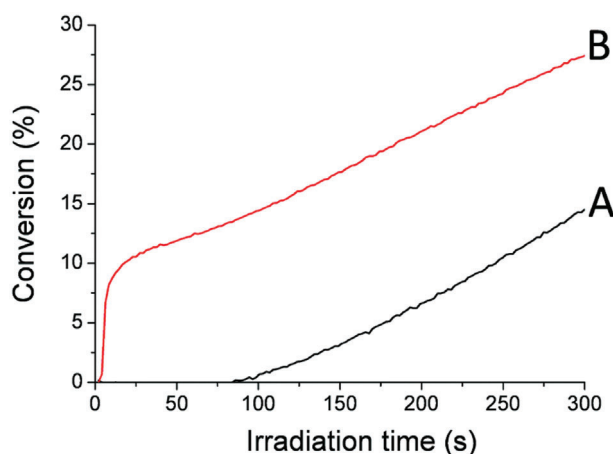


Figure 9. Polymerization profiles of TMPTA upon Hg-Xe lamp irradiation under air in the presence of A) DMPA (1% wt) and B) DMPA/**Zn-4** (1%/0.3%, w/w). Reproduced with permission.^[98] Copyright 2014, Royal Society of Chemistry.

trolled by changing the irradiation wavelengths, as **Zn-5** shows absorptions at 520, 570, and 600 nm. This aspect is typically regulated by acting on light intensity or catalyst concentration. Using 100 ppm of **Zn-5**, conversions of 90% for MMA were achieved in the presence of CDTPA and blue LED irradiation (435–480 nm) after 12 h. After 2 h, similar results were obtained with MA in the presence of BTPA and red-light irradiation (610–655 nm).^[99] Using the same **Zn-5** complex, good conversions were obtained using *ortho*-substituted methacrylates, such as *o*-nitrobenzyl methacrylate (NBMA). It is worth mentioning that the polymerization of this type of monomer is often challenging due to the nitro substituent that inhibits or delays the normal FRP, determining low conversions and broad polymer dispersity. Instead, using CDTPA and yellow ($\lambda_{\text{max}} = 560 \text{ nm}$) or red ($\lambda_{\text{max}} = 635 \text{ nm}$) light irradiation, the corresponding PET-RAFT homopolymer was prepared with well-defined molecular weight and polymer dispersity.^[100] **Zn-5** was applied by Lalevée and coworkers for FRP of methacrylates and ROP of EPOX under air and upon LED exposure at 405, 455, 477, and 530 nm. As concerns, the former, BisGMA and TEGDMA, were exploited as monomers in 1.4 mm thick films. The best performances were achieved using LED@477 nm and LED@530 nm, where 70% and 50% conversions were detected after 100 s irradiation. Instead, conversions of EPOX (25 μm thick film) over 30% were obtained after 800 s of irradiation (LED@405 nm, LED@455 nm, and LED@530 nm) in two-component systems in the presence of Iod (**Zn-5**/Iod, 0.3%/1% w/w). In both cases, no polymerization was observed using only the ligand in combination with Iod (0.5%/1%, w/w), indicating the key role played by the metal center. This system was also tested for the 3D printing of EPOX under air, using **Zn-5**/Iod (0.3%/1% w/w) and LED@405 nm. Different patterns could be obtained with relatively low light intensity ($I \approx 100\text{--}130 \text{ mW cm}^{-2}$) owing to the good performances of the proposed method (see, for instance, the numbers and the patterns reported in Figure 10).^[101] More recently, **Zn-5** was employed for the FRP of TMPTA and MA in absence of co-initiators, additives or RAFT agents, exploiting two-photon absorption processes and a laser diode at 561 nm ($I \approx 10^5 \text{ W cm}^{-2}$).^[34b]

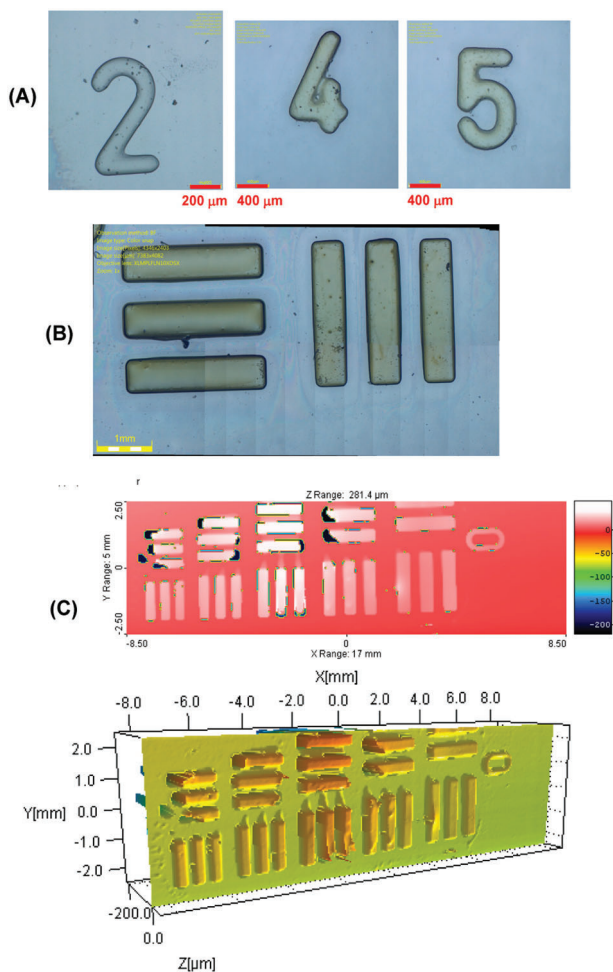


Figure 10. A) and B): different numbers (2, 4, 5) and patterns prepared by 3D photopolymerization technique using LED@405 nm. C): characterization of the patterns via profilometry experiments. Reproduced with permission.^[101] Copyright 2017, American Chemical Society.

5. Bimetallic Complexes in Photoinitiating Systems

As previously described, long excited-state lifetimes are critical to obtain good photopolymerization performances. One approach to further extend this feature and the absorption properties relies on using bimetallic complexes. Lalevée and coworkers reported the bimetallic complex **Ru-Ir** sketched in **Scheme 18** that was tested for the photopolymerization of an NVC/EPOX film (50%/50% w/w) under blue LED irradiation ($\lambda = 462$ nm) in the presence of TTMS and Ph_2I^+ (0.2%/3%/2% w/w). The complex exhibited longer lifetimes than **Ir-4** and **Ir-5**, affording conversions of over 70% after 400 s. Just like **Ir-4**, the homopolymerization of NVC in aerated toluene (50%/50% w/w) and under halogen lamp irradiation ($\lambda > 400$ nm) was almost immediate, and complete conversions were detected after less than 3 s of irradiation.^[78]

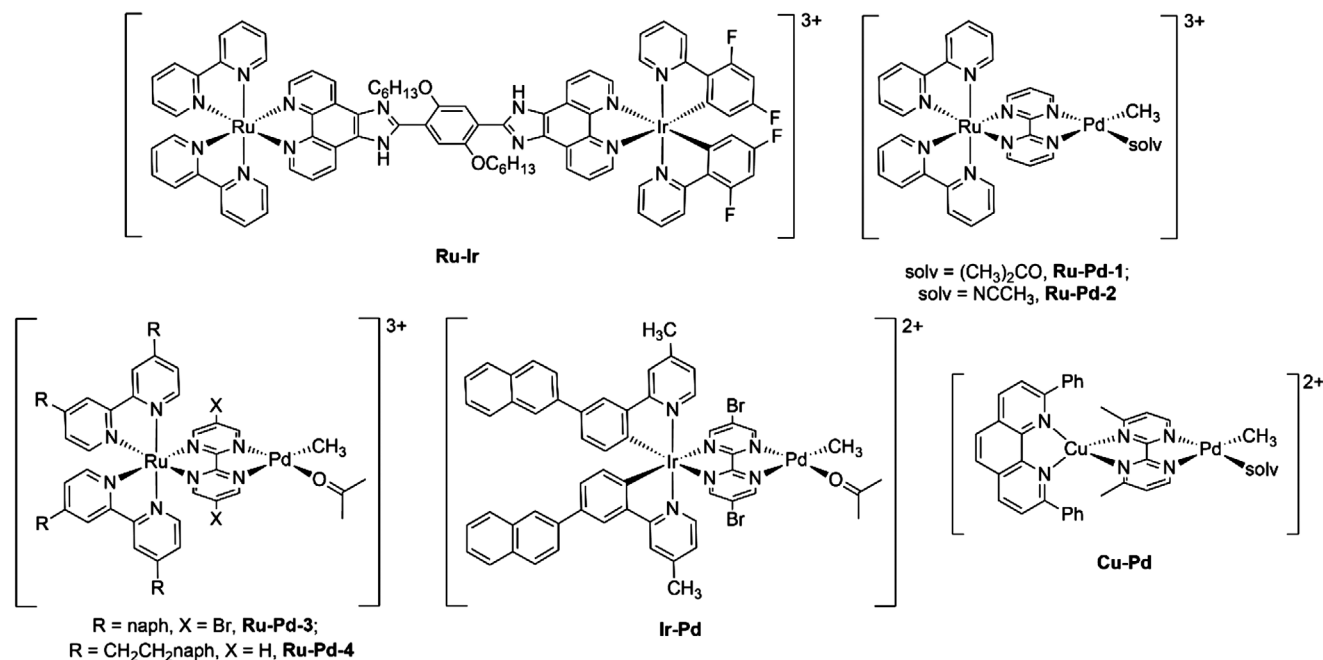
Another method to increase the absorption and emissive features is using bichromophoric systems in which extended π -aromatic groups are directly linked to bpy, ppy, or phen ligands. Bichromophoric complexes composed of Ru(II), Ir(III) or Cu(I),

and Pd(II) combine the ability of the former to absorb and transfer light, with the capacity of the latter to propagate the polymeric chain. As previously stated, Pd(II) complexes are widely applied to polymerize olefins.^[79] Light irradiation can help to achieve unique architectures that cannot be realized with standard polymerization techniques. For instance, the bichromophoric Ru-Pd complexes with bipyridyl (bpy) and bipyrimidinyl (bpm) ligands **Ru-Pd-1** and **Ru-Pd-2** were active toward the dimerization of styrene to 2,4-diphenyl-4-methyl-1-pentene under visible-light irradiation (150 W Xe lamp, $\lambda > 420$ nm). The reaction did not proceed in the dark without a photocatalyst, even after 30 h. Instead, 1 mol.% of the photocatalyst was sufficient to afford the dimer in 90% yield. Based on computational calculations, Ru(II) has a key role in the excitation of Pd-alkyl intermediates by accelerating the second insertion of α -methylstyrene, which is the rate-determining step of the overall catalytic cycle (see **Scheme 19**).^[102]

When **Ru-Pd-3** and **Ru-Pd-4** were employed in the photoinitiating systems, different products were obtained under the same experimental conditions. **Ru-Pd-3** selectively catalyzed the formation of polystyrene but with conversion under 40% after 12 h due to the decomposition of the catalyst. On the other hand, **Ru-Pd-4** behaved like the previously described **Ru-Pd-1** and **Ru-Pd-2**, catalyzing the dimerization of styrene. The different catalytic activity can be ascribed to the photophysical properties of the two complexes. More in detail, for **Ru-Pd-4**, the lifetime decay curve is monoexponential, with $\tau \approx 60$ ns; for **Ru-Pd-3**, it is biexponential with one value ≈ 90 ns (for 73%) and the other one close to 1 μs (for the 27%). The second value is probably connected to the antenna effect of the naphthyl moiety directly bonded to the bpy ligand, which is able to absorb UV light and then transfer it to Ru(II), thus increasing the luminescent lifetimes owing to a more efficient metal-to-ligand charge transfer (MLCT).^[103]

A similar bichromophoric system was prepared using Ir(III) in combination with the previously reported {Pd}-fragment. Similarly to the previously described complexes, **Ir-Pd** was active toward the polymerization of styrene under visible light irradiation affording high molecular weight polystyrene. The reaction proceeded even when 2,6-di-*tert*-butyl-4-methylphenol (BHT) was used as a radical scavenger, suggesting that a nonradical polymerization mechanism was involved. It is widely known that styrene derivatives bearing an electron-withdrawing group are usually characterized by low reactivity. The homopolymerization of 4-chlorostyrene (4-Cl-St) with 1 mol.% of **Ir-Pd** did not occur in dark conditions, but under $\lambda > 420$ nm conversions $\approx 30\%$ were detected after 24 h. Similar results were achieved with the copolymerization of styrene and 4-Cl-St (50%/50%, w/w).^[104] The same complex **Ir-Pd** (0.5–1 mol.%) was also active toward the homopolymerization of 2,2,2-trifluoroethyl vinyl ether (TFEVE) and pentafluorobenzyl vinyl ether (PFBnVE), both under light and in the dark. The results obtained with the two types of monomers were extended to the copolymerization reaction of styrene with vinyl ethers. Also, in this case, the coordination-insertion mechanism appears to be accelerated by light since the copolymerization reaction was slowed down in dark conditions affording, for instance, only the dimerization of styrene when it was used as a monomer together with TFEVE.^[105]

To prepare a more sustainable bichromophoric PI, Cu(I) was used instead of the precious Ru(II) or Ir(III) to afford a family



Scheme 18. Selected bimetallic complexes applied in photopolymerizations.

of Cu-Pd dimers that were tested for the photopolymerization of 4-Ome-St under blue light ($\lambda = 420$ nm). **Cu-Pd** exhibited the best photocatalytic performances affording 98% conversion for the corresponding polystyrene after 4 h of irradiation. Similarly to what was observed for other bichromophoric systems, the conversion was only $\approx 4\%$ in the dark, suggesting that both photocatalyst and light are required for the process. Investigations on the two separate complexes revealed that the Pd(II) derivative could catalyze the photopolymerization with conversions $\approx 98\%$. However, photodecomposition was also detected, and it is supposed that the Pd species formed during this process were responsible for the polymerization of 4-Ome-St. In addition, the polymerization proceeded even in the presence of high amounts (10 equivalents) of commonly used radical and cation scavengers, such as the previously mentioned BHT, TEMPO, or 2,6-di-*tert*-butylpyridine. Nevertheless, it is worth noting that the reaction slowed down, and only 47–48% conversions were detected using TEMPO and 2,6-di-*tert*-butylpyridine after 4 h of photoirradiation. Following these considerations, the Cu(I) fragment behaves like Ru(II) in Ru-Pd systems, accelerating the coordination-insertion mechanism through a non-radical mechanism.^[106]

6. Conclusion

The ability of transition metal complexes to generate radicals when exposed to light irradiation has been known since the Sixties. After that, several complexes were tested in radical and cationic photopolymerizations as PIs and PSs. The former are generally organometallic derivatives with the metal-carbon bonds that can easily be broken by light irradiation, whereas the latter are normally characterized by extended π -conjugated ligands and emissions originating from charge transfer processes. Transition metal complexes generally work in two- or three-component sys-

tems, determining, in some cases, comparable performances or even improved conversions if compared to organic fluorophores owing to their strong absorptions, long-lived triplet excited states and reversible redox potentials. However, the investigation of transition metal complexes applied to 3D printing is still in its early stages. Due to the risks and high energetic demands of UV light, visible light irradiation from LED to household lamps should be preferred, but photoinitiating systems working in the visible range (from green to NIR) are still rare compared to blue/UV light systems currently exploited for 3D printing. Two-photon absorption can be potentially employed for such purposes, allowing the use of less harmful irradiation, although its application is currently limited to lasers as light sources due to the high light power required. In conclusion, all these aspects should be considered when modelling the next generation of transition metal-based photoinitiating systems in combination with sustainability factors linked to using earth-abundant elements.

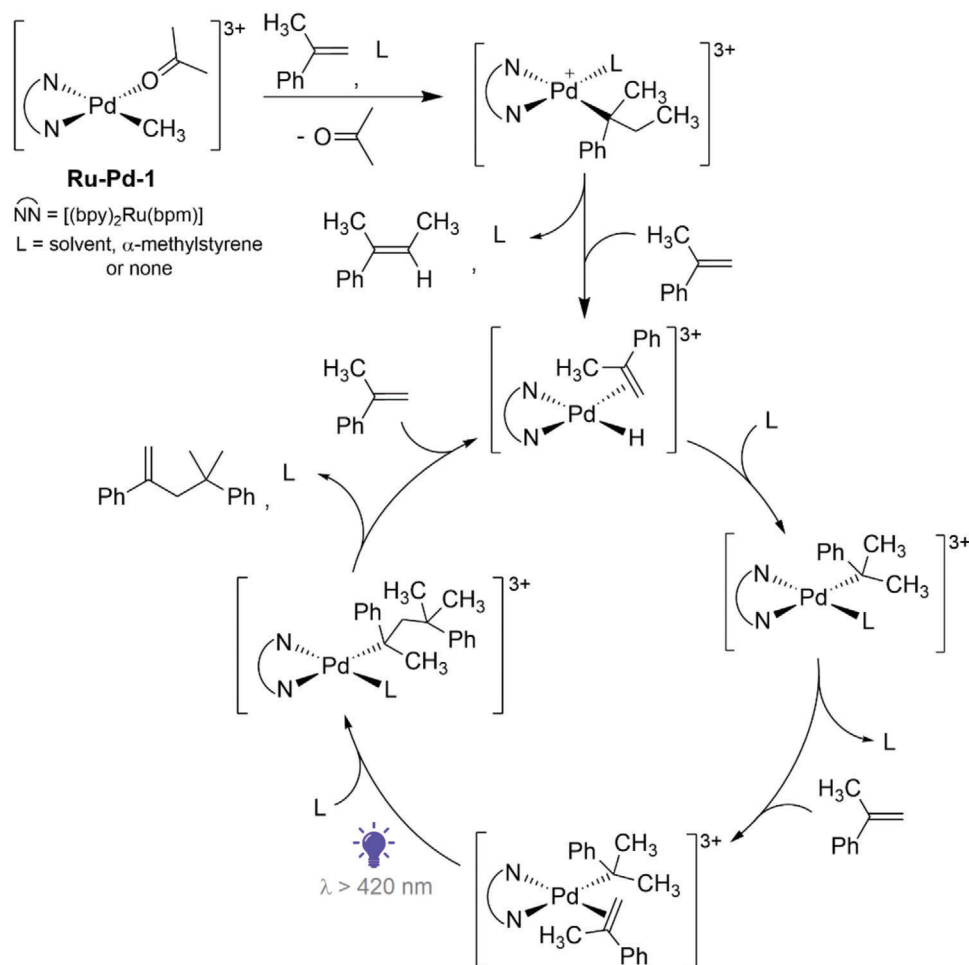
Acknowledgements

This research had been funded by the Deutsche Forschungsgemeinschaft (DFG, German Research Foundation) under Germany's Excellence Strategy via the Excellence Cluster "3D Matter Made to Order" (3DMM2O, EXC-2082/1-390761711, Thrust A1 and A3). The authors further acknowledge support from the Karlsruhe School of Optics & Photonics (KSOP) and Graduate Funding from the German States.

Open access funding enabled and organized by Projekt DEAL.

Conflict of Interest

The authors declare no conflict of interest.



Scheme 19. Proposed mechanism for the dimerization of α -methylstyrene.

Keywords

3D printing, photoinitiators, photopolymerization, photosensitizers, transition metal complexes

Received: February 23, 2023

Revised: April 24, 2023

Published online:

- [1] V. Balzani, P. Ceroni, A. Juris, *Photochemistry and Photophysics: Concepts, Research, Applications*, Wiley, Hoboken, NJ **2014**.
 [2] A. J. Teator, D. N. Lastovickova, C. W. Bielawski, *Chem. Rev.* **2016**, *116*, 1969.
 [3] T. Pirman, M. Ocepek, B. Likozar, *Ind. Eng. Chem. Res.* **2021**, *60*, 9347.
 [4] a) A. Bagheri, J. Jin, *ACS Appl Polym Mater* **2019**, *1*, 593; b) Y. Yagci, S. Jockusch, N. J. Turro, *Macromolecules* **2010**, *43*, 6245; c) Z. A. Matthew, R. Hartings, *Nat. Rev. Chem.* **2019**, *3*, 305; d) S. Chatani, C. J. Kloxin, C. N. Bowman, *Polym. Chem.* **2014**, *5*, 2187; e) N. Moszner, U. Salz, *Macromol. Mater. Eng.* **2007**, *292*, 245.
 [5] a) F. Jasinski, P. B. Zetterlund, A. M. Braun, A. Chemtob, *Prog. Polym. Sci.* **2018**, *84*, 47; b) X. Pan, M. A. Tasdelen, J. Laun, T. Junkers, Y. Yagci, K. Matyjaszewski, *Prog. Polym. Sci.* **2016**, *62*, 73; c) C. Wu, N.

Corrigan, C.-H. Lim, W. Liu, G. Miyake, C. Boyer, *Chem. Rev.* **2022**, *122*, 5476; d) R. D. M. Kira Behm, *ChemPlusChem* **2020**, *85*, 2611.

- [6] G. Noirbent, F. Dumur, *Catalysts* **2020**, *10*, 953.
 [7] A. H. Bonardi, F. Dumur, T. M. Grant, G. Noirbent, D. Gigmes, B. H. Lessard, J. P. Fouassier, J. Lalevée, *Macromolecules* **2018**, *51*, 1314.
 [8] a) M. Kaur, A. K. Srivastava, *J. Macromol. Sci., Pol. R.* **2002**, *42*, 481; b) A. M. Doerr, J. M. Burroughs, S. R. Gitter, X. Yang, A. J. Boydston, B. K. Long, *ACS Catal.* **2020**, *10*, 14457; c) J.-P. Fouassier, J. Lalevée, *Photoinitiators: Structures, Reactivity and Applications in Polymerization*, Wiley, Weinheim, Germany **2021**.
 [9] a) J.-P. Fouassier, F. Morlet-Savary, J. Lalevée, X. Allonas, C. Ley, *Materials* **2010**, *3*, 5130; b) A. Balcerak, J. Kabatc, *RSC Adv.* **2019**, *9*, 28490; c) N. Zivic, M. Bouzrati-Zerelli, A. Kermagoret, F. Dumur, J.-P. Fouassier, D. Gigmes, J. Lalevée, *ChemCatChem* **2016**, *8*, 1617.
 [10] N. M. Bojanowski, A. Vranic, V. Hahn, P. Rietz, T. Messer, J. Brückel, C. Barner-Kowollik, E. Blasco, S. Bräse, M. Wegener, *Adv. Funct. Mater.* **2022**, 2212482.
 [11] K. Sun, P. Xiao, F. Dumur, J. Lalevée, *J. Polym. Sci.* **2021**, *59*, 1338.
 [12] C. K. Prier, D. A. Rankic, D. W. MacMillan, *Chem. Rev.* **2013**, *113*, 5322.
 [13] F. A. Leibfarth, K. M. Mattson, B. P. Fors, H. A. Collins, C. J. Hawker, *Angew. Chem., Int. Ed.* **2013**, *52*, 199.
 [14] P. Weiss, *Pure Appl. Chem.* **1967**, *15*, 587.
 [15] P. Xiao, J. Zhang, F. Dumur, M. A. Tehfe, F. Morlet-Savary, B. Graff, D. Gigmes, J. P. Fouassier, J. Lalevée, *Prog. Polym. Sci.* **2015**, *41*, 32.

- [16] M. Sangermano, N. Razza, J. V. Crivello, *Macromol. Mater. Eng.* **2014**, 299, 775.
- [17] a) M. A. Tasdelen, M. Uygun, Y. Yagci, *Macromol. Chem. Phys.* **2010**, 211, 2271; b) M. Chen, M. Zhong, J. A. Johnson, *Chem. Rev.* **2016**, 116, 10167.
- [18] K. V. Wong, A. Hernandez, *ISRN Mech. Eng.* **2012**, 2012, 1.
- [19] V. Hahn, P. Kiefer, T. Frenzel, J. Qu, E. Blasco, C. Barner-Kowollik, M. Wegener, *Adv. Funct. Mater.* **2020**, 30, 1907795.
- [20] Y. Bao, *Macromol. Rapid Commun.* **2022**, 43, 2200202.
- [21] J. Shao, Y. Huang, Q. Fan, *Polym. Chem.* **2014**, 5, 4195.
- [22] D. A. Bolon, K. K. Webb, *J. Appl. Polym. Sci.* **1978**, 22, 2543.
- [23] a) C. A. Spiegel, M. Hackner, V. P. Bothe, J. P. Spatz, E. Blasco, *Adv. Funct. Mater.* **2022**, 32, 2110580; b) L. Breloy, V. Brezová, Z. Barbieriková, Y. Ito, J. Akimoto, A. Chiappone, S. Abbad-Andaloussi, J.-P. Malval, D.-L. Versace, *ACS Appl Polym Mater* **2022**, 4, 210; c) F. Kotz, K. Arnold, W. Bauer, D. Schild, N. Keller, K. Sachsenheimer, T. M. Nargang, C. Richter, D. Helmer, B. E. Rapp, *Nature* **2017**, 544, 337.
- [24] M. Göppert-Mayer, *Ann. Phys.* **1931**, 401, 273.
- [25] V. Hahn, N. M. Bojanowski, P. Rietz, F. Feist, M. Kozłowska, W. Wenzel, E. Blasco, S. Bräse, C. Barner-Kowollik, M. Wegener, *ACS Photonics* **2023**, 10, 24.
- [26] V. Hahn, T. Messer, N. M. Bojanowski, E. R. Curticean, I. Wacker, R. R. Schröder, E. Blasco, M. Wegener, *Nat. Photon.* **2021**, 15, 932.
- [27] C. Walling, M. J. Gibian, *J. Am. Chem. Soc.* **1965**, 87, 3361.
- [28] a) L. J. Johnston, M. Tencer, J. C. Scaiano, *J. Org. Chem.* **1986**, 51, 2806; b) T. Ito, F. W. Seidel, X. Jin, K. Nozaki, *J. Org. Chem.* **2022**, 87, 12733.
- [29] V. Hahn, F. Mayer, M. Thiel, M. Wegener, *Opt Photonics News* **2019**, 30, 28.
- [30] Y. Lin, J. Xu, *Adv. Opt. Mater.* **2018**, 6, 1701359.
- [31] D. Mandt, P. Gruber, M. Markovic, M. Tromayer, M. Rothbauer, S. R. A. Kratz, S. F. Ali, J. V. Hoorick, W. Holnthoner, S. Mühleder, P. Dubruel, S. V. Vlierbergh, P. Ertl, R. Liska, A. Ovsianikov, *Int. J. Bio-printing* **2018**, 4, 144.
- [32] X. Wang, Z. Wei, C. Z. Baysah, M. Zheng, J. Xing, *RSC Adv.* **2019**, 9, 34472.
- [33] D. K. Limberg, J.-H. Kang, R. C. Hayward, *J. Am. Chem. Soc.* **2022**, 144, 5226.
- [34] a) S. N. Sanders, T. H. Schloemer, M. K. Gangishetty, D. Anderson, M. Seitz, A. O. Gallegos, R. C. Stokes, D. N. Congreve, *Nature* **2022**, 604, 474; b) N. Awwad, A. T. Bui, E. O. Danilov, F. N. Castellano, *Chem* **2020**, 6, 3071.
- [35] a) H. A. Skinner, J. A. Connor, *Pure Appl. Chem.* **1985**, 57, 79; b) E. Riedel, H.-J. Meyer, *Allgemeine und Anorganische Chemie*, xx, De Gruyter **2018**.
- [36] a) K. Kaeriyama, Y. Shimura, *J. Polym. Sci., Part A: Polym. Chem.* **1972**, 10, 2833; b) C. H. Bamford, R. Denyer, *Nature* **1968**, 217, 59; c) C. H. Bamford, P. A. Crowe, R. P. Wayne, *Proc. R. Soc. Lond. A Mat* **1965**, 284, 455.
- [37] S. Dadashi-Silab, S. Doran, Y. Yagci, *Chem. Rev.* **2016**, 116, 10212.
- [38] F. Dumur, *Catalysts* **2019**, 9.
- [39] J. Lalevé, N. Blanchard, M.-A. Tehfe, F. Morlet-Savary, J. P. Fouassier, *Macromolecules* **2010**, 43, 10191.
- [40] W. Kaminsky, *Polyolefins: 50 Years after Ziegler and Natta II: Polyolefins by Metallocenes and Other Single-Site Catalysts*, Springer, Heidelberg, Germany **2013**.
- [41] a) K. Meier, *Coord. Chem. Rev.* **1991**, 111, 97; b) K. Bukovinsky, M. Szalóki, I. Csarnovics, I. Szabó, S. Kéki, M. Nagy, C. Hegedűs, *Adv. Condens. Matter Phys.* **2018**, 2018, 1.
- [42] a) M.-A. Tehfe, J. Lalevé, F. Morlet-Savary, B. Graff, J.-P. Fouassier, *Macromolecules* **2012**, 45, 356; b) M. A. Tehfe, J. Lalevé, X. Allonas, J. P. Fouassier, *Macromolecules* **2009**, 42, 8669.
- [43] J. Lalevé, M.-A. Tehfe, D. Gímes, J. P. Fouassier, *Macromolecules* **2010**, 43, 6608.
- [44] M. Ciftci, M. A. Tasdelen, Y. Yagci, *Polym. Chem.* **2014**, 5, 600.
- [45] M. A. Tehfe, J. Lalevé, D. Gímes, J. P. Fouassier, *J. Polym. Sci., Part A: Polym. Chem.* **2010**, 48, 1830.
- [46] H. Chen, Y. Zhang, A. Bonfiglio, F. Morlet-Savary, M. Mauro, J. Lalevé, *ACS Appl Polym Mater* **2021**, 3, 464.
- [47] a) F. Dumur, *Eur. Polym. J.* **2021**, 147, 110328; b) F. Dumur, *Eur. Polym. J.* **2020**, 139.
- [48] B. Zhao, J. Li, X. Pan, Z. Zhang, G. Jin, J. Zhu, *ACS Macro Lett.* **2021**, 10, 1315.
- [49] a) J. Zhang, D. Campolo, F. Dumur, P. Xiao, J. P. Fouassier, D. Gímes, J. Lalevé, *J. Polym. Sci., Part A: Polym. Chem.* **2015**, 53, 42; b) J. Zhang, D. Campolo, F. Dumur, P. Xiao, J. P. Fouassier, D. Gímes, J. Lalevé, *ChemCatChem* **2016**, 8, 2227.
- [50] J. Zhang, D. Campolo, F. Dumur, P. Xiao, J. P. Fouassier, D. Gímes, J. Lalevé, *J. Polym. Sci., Part A: Polym. Chem.* **2016**, 54, 2247.
- [51] a) C. K. Prier, D. A. Rankic, D. W. C. Macmillan, *Chem. Rev.* **2013**, 113, 5322; b) J. D. Nguyen, E. M. D'Amato, J. M. R. Narayanam, C. R. J. Stephenson, *Nat. Chem.* **2012**, 4, 854; c) C.-J. Wallentin, J. D. Nguyen, P. Finkbeiner, C. R. J. Stephenson, *J. Am. Chem. Soc.* **2012**, 134, 8875.
- [52] J. Xu, A. Atme, A. F. Marques Martins, K. Jung, C. Boyer, *Polym. Chem.* **2014**, 5, 3321.
- [53] K. Iwai, M. Uesugi, F. Takemura, *Polym J* **1985**, 17, 1005.
- [54] Y. Chen, Z. Hu, D. Xu, Y. Yu, X. Tang, H. Guo, *Macromol. Chem. Phys.* **2015**, 216, 1055.
- [55] G. Zhang, I. Y. Song, K. H. Ahn, T. Park, W. Choi, *Macromolecules* **2011**, 44, 7594.
- [56] G. Zhang, I. Y. Song, T. Park, W. Choi, *Green Chem.* **2012**, 14, 618.
- [57] J. Xu, K. Jung, N. A. Corrigan, C. Boyer, *Chem. Sci.* **2014**, 5, 3568.
- [58] K. S. Lim, B. S. Schon, N. V. Mekhileri, G. C. J. Brown, C. M. Chia, S. Prabakar, G. J. Hooper, T. B. F. Woodfield, *ACS Biomater. Sci. Eng.* **2016**, 2, 1752.
- [59] X. Xu, A. Seijo-Rabina, A. Awad, C. Rial, S. Gaisford, A. W. Basit, A. Goyanes, *Int. J. Pharm.* **2021**, 609, 121199.
- [60] W. Li, M. Wang, L. S. Mille, J. A. Robledo Lara, V. Huerta, T. Uribe Velázquez, F. Cheng, H. Li, J. Gong, T. Ching, C. A. Murphy, A. Lesha, S. Hassan, T. B. F. Woodfield, K. S. Lim, Y. S. Zhang, *Adv. Mater.* **2021**, 33, 2102153.
- [61] J. Lalevé, N. Blanchard, M.-A. Tehfe, M. Peter, F. Morlet-Savary, D. Gímes, J. P. Fouassier, *Polym. Chem.* **2011**, 2, 1986.
- [62] J. Lalevé, S. Telitel, P. Xiao, M. Lepeltier, F. Dumur, F. Morlet-Savary, D. Gímes, J.-P. Fouassier, *Beilstein J. Org. Chem.* **2014**, 10, 863.
- [63] J. Lalevé, N. Blanchard, M.-A. Tehfe, M. Peter, F. Morlet-Savary, J. P. Fouassier, *Polym. Bull.* **2012**, 68, 341.
- [64] N. V. Alfredo, N. E. Jalapa, S. L. Morales, A. D. Ryabov, R. Le Lagadec, L. Alexandrova, *Macromolecules* **2012**, 45, 8135.
- [65] D.-L. Versace, J. Cerezo Bastida, C. Lorenzini, C. Cachet-Vivier, E. Renard, V. Langlois, J.-P. Malval, J.-P. Fouassier, J. Lalevé, *Macromolecules* **2013**, 46, 8808.
- [66] a) C.-H. Peng, S. Li, B. B. Wayland, *J. Chin Chem Soc* **2009**, 56, 219; b) C.-M. Liao, C.-C. Hsu, F.-S. Wang, B. B. Wayland, C.-H. Peng, *Polym. Chem.* **2013**, 4, 3098; c) C.-S. Hsu, T.-Y. Yang, C.-H. Peng, *Polym. Chem.* **2014**, 5, 3867; d) F.-S. Wang, S.-H. Lin, G.-H. Zheng, M.-H. Li, Y.-C. Cheng, C.-H. Peng, *Macromolecules* **2022**, 55, 4276.
- [67] Y. Zhao, M. Yu, X. Fu, *Chem. Commun.* **2013**, 49, 5186.
- [68] Y. Zhao, M. Yu, S. Zhang, Y. Liu, X. Fu, *Macromolecules* **2014**, 47, 6238.
- [69] B. P. Fors, C. J. Hawker, *Angew. Chem., Int. Ed.* **2012**, 51, 8850.
- [70] N. J. Treat, B. P. Fors, J. W. Kramer, M. Christianson, C.-Y. Chiu, J. Read De Alaniz, C. J. Hawker, *ACS Macro Lett.* **2014**, 3, 580.
- [71] X. Liu, Y. Ni, J. Wu, H. Jiang, Z. Zhang, L. Zhang, Z. Cheng, X. Zhu, *Polym. Chem.* **2018**, 9, 584.

- [72] J. Lalevée, N. Blanchard, M.-A. Tehfe, M. Peter, F. Morlet-Savary, J. P. Fouassier, *Macromol. Rapid Commun.* **2011**, *32*, 917.
- [73] a) J. Lalevée, M. Peter, F. Dumur, D. Gigmes, N. Blanchard, M.-A. Tehfe, F. Morlet-Savary, J. P. Fouassier, *Chem. - Eur. J.* **2011**, *17*, 15027; b) S. Telitel, F. Dumur, M. Lepeltier, D. Gigmes, J. P. Fouassier, J. Lalevée, *C. R. Chim.* **2016**, *19*, 71.
- [74] J. Xu, K. Jung, A. Atme, S. Shanmugam, C. Boyer, *J. Am. Chem. Soc.* **2014**, *136*, 5508.
- [75] S. Shanmugam, J. Xu, C. Boyer, *Macromolecules* **2014**, *47*, 4930.
- [76] J. Lalevée, M.-A. Tehfe, F. Dumur, D. Gigmes, N. Blanchard, F. Morlet-Savary, J. P. Fouassier, *ACS Macro Lett.* **2012**, *1*, 286.
- [77] S. Telitel, F. Dumur, S. Telitel, O. Soppera, M. Lepeltier, Y. Guillaneuf, J. Poly, F. Morlet-Savary, P. Fioux, J.-P. Fouassier, D. Gigmes, J. Lalevée, *Polym. Chem.* **2015**, *6*, 613.
- [78] J. Lalevée, F. Dumur, C. R. Mayer, D. Gigmes, G. Nasr, M.-A. Tehfe, S. Telitel, F. Morlet-Savary, B. Graff, J. P. Fouassier, *Macromolecules* **2012**, *45*, 4134.
- [79] C. S. P. Zhibin Guan, *Recent Progress in Late Transition Metal α -Diimine Catalysts for Olefin Polymerization*, Springer, Heidelberg, Germany **2009**.
- [80] M. Li, R. Wang, M. S. Eisen, S. Park, *Org. Chem. Front.* **2020**, *7*, 2088.
- [81] C. Son, A. Inagaki, *Dalton Trans.* **2016**, *45*, 1331.
- [82] A. Keyes, H. E. Basbug Alhan, U. Ha, Y.-S. Liu, S. K. Smith, T. S. Teets, D. B. Beezer, E. Harth, *Macromolecules* **2018**, *51*, 7224.
- [83] M.-A. Tehfe, L. Ma, B. Graff, F. Morlet-Savary, J.-P. Fouassier, J. Zhao, J. Lalevée, *Macromol. Chem. Phys.* **2012**, *213*, 2282.
- [84] a) A. Anastasaki, V. Nikolaou, Q. Zhang, J. Burns, S. R. Samanta, C. Waldron, A. J. Haddleton, R. McHale, D. Fox, V. Percec, P. Wilson, D. M. Haddleton, *J. Am. Chem. Soc.* **2014**, *136*, 1141; b) A. Anastasaki, V. Nikolaou, A. Simula, J. Godfrey, M. Li, G. Nurumbetov, P. Wilson, D. M. Haddleton, *Macromolecules* **2014**, *47*, 3852; c) D. Konkolewicz, K. Schröder, J. Buback, S. Bernhard, K. Matyjaszewski, *ACS Macro Lett.* **2012**, *1*, 1219; d) T. Zhang, T. Chen, I. Amin, R. Jordan, *Polym. Chem.* **2014**, *5*, 4790; e) T. G. Ribelli, D. Konkolewicz, X. Pan, K. Matyjaszewski, *Macromolecules* **2014**, *47*, 6316.
- [85] P. Xiao, J. Zhang, D. Campolo, F. Dumur, D. Gigmes, J. P. Fouassier, J. Lalevée, *J. Polym. Sci., Part A: Polym. Chem.* **2015**, *53*, 2673.
- [86] D. V. Scaltrito, D. W. Thompson, J. A. O'Callaghan, G. J. Meyer, *Coord. Chem. Rev.* **2000**, *208*, 243.
- [87] Q. Yang, F. Dumur, F. Morlet-Savary, J. Poly, J. Lalevée, *Macromolecules* **2015**, *48*, 1972.
- [88] P. Xiao, F. Dumur, J. Zhang, J. P. Fouassier, D. Gigmes, J. Lalevée, *Macromolecules* **2014**, *47*, 3837.
- [89] P. Garra, F. Dumur, D. Gigmes, A. Al Mousawi, F. Morlet-Savary, C. Dietlin, J. P. Fouassier, J. Lalevée, *Macromolecules* **2017**, *50*, 3761.
- [90] P. Xiao, F. Dumur, J. Zhang, D. Gigmes, J. P. Fouassier, J. Lalevée, *Polym. Chem.* **2014**, *5*, 6350.
- [91] M. Bouzrati-Zerelli, N. Guillaume, F. Goubard, T.-T. Bui, S. Villotte, C. Dietlin, F. Morlet-Savary, D. Gigmes, J. P. Fouassier, F. Dumur, J. Lalevée, *New J. Chem.* **2018**, *42*, 8261.
- [92] a) H. Yiersin, *Highly Efficient OLEDs: Materials Based on Thermally Activated Delayed Fluorescence*, Wiley, Weinheim, Germany **2019**; b) G. Hong, X. Gan, C. Leonhardt, Z. Zhang, J. Seibert, J. M. Busch, S. Bräse, *Adv. Mater.* **2021**, *33*, 2005630; c) R. Czerwieniec, M. J. Leitl, H. H. H. Homeier, H. Yersin, *Coord. Chem. Rev.* **2016**, *325*, 2.
- [93] A. Al Mousawi, A. Kermagoret, D.-L. Versace, J. Toufaily, T. Hamieh, B. Graff, F. Dumur, D. Gigmes, J. P. Fouassier, J. Lalevée, *Polym. Chem.* **2017**, *8*, 568.
- [94] F. Hammoud, M. Rahal, J. Egly, F. Morlet-Savary, A. Hijazi, S. Bellemin-Laponnaz, M. Mauro, J. Lalevée, *Polym. Chem.* **2021**, *12*, 2848.
- [95] M. Rahal, G. Noirbent, B. Graff, J. Toufaily, T. Hamieh, D. Gigmes, F. Dumur, J. Lalevée, *Polymers* **2022**, *14*, 1998.
- [96] F. Nzulu, S. Telitel, F. Stoffelbach, B. Graff, F. Morlet-Savary, J. Lalevée, L. Fensterbank, J.-P. Goddard, C. Ollivier, *Polym. Chem.* **2015**, *6*, 4605.
- [97] M.-A. Tehfe, F. Dumur, S. Telitel, D. Gigmes, E. Contal, D. Bertin, F. Morlet-Savary, B. Graff, J.-P. Fouassier, J. Lalevée, *Eur. Polym. J.* **2013**, *49*, 1040.
- [98] D. L. Versace, J. Bourgon, E. Leroy, F. Dumur, D. Gigmes, J. P. Fouassier, J. Lalevée, *Polym. Chem.* **2014**, *5*, 6569.
- [99] S. Shanmugam, J. Xu, C. Boyer, *J. Am. Chem. Soc.* **2015**, *137*, 9174.
- [100] A. Bagheri, J. Yeow, H. Arandiyani, J. Xu, C. Boyer, M. Lim, *Macromol. Rapid Commun.* **2016**, *37*, 905.
- [101] A. Al Mousawi, C. Poriel, F. Dumur, J. Toufaily, T. Hamieh, J. P. Fouassier, J. Lalevée, *Macromolecules* **2017**, *50*, 746.
- [102] a) A. Inagaki, S. Edure, S. Yatsuda, M. Akita, *Chem. Commun.* **2005**, 5468; b) K. Murata, A. Inagaki, M. Akita, J.-F. Halet, K. Costuas, *Inorg. Chem.* **2013**, *52*, 8030.
- [103] a) K. Murata, M. Ito, A. Inagaki, M. Akita, *Chem. Lett.* **2010**, *39*, 915; b) H. Nitadori, T. Takahashi, A. Inagaki, M. Akita, *Inorg. Chem.* **2012**, *51*, 51; c) K. Murata, M. Araki, A. Inagaki, M. Akita, *Dalton Trans.* **2013**, *42*, 6989.
- [104] R. Ohyama, M. Mishima, A. Inagaki, *Dalton Trans.* **2021**, *50*, 12716.
- [105] S. Kikuchi, K. Saito, M. Akita, A. Inagaki, *Organometallics* **2018**, *37*, 359.
- [106] T. Fujiwara, K. Nomura, A. Inagaki, *Organometallics* **2020**, *39*, 2464.



Valentina Ferraro received her B.Sc. and M.Sc. degrees in Chemistry and Sustainable Technologies from Ca' Foscari University of Venice (Italy). She completed her Ph.D. in Chemistry under the supervision of Prof. Marco Bortoluzzi in 2022 in a joint program between the University of Trieste and Ca' Foscari University of Venice. She is currently a postdoctoral researcher in Prof. Bräse's group under the 3DMM2O cluster (Thrust A1), focusing on luminescent Cu(I) complexes to be applied as photoinitiators for 3D printing.



Clara R. Adam received her B.Sc. and M.Sc. degrees in Chemistry from the Karlsruhe Institute of Technology (Germany). She currently works on her Ph.D. in organic chemistry in the group of Prof. Stefan Bräse, founded by Graduate Funding from the German States (LGF) and focusing on luminescent Cu(I) complexes as TADF emitters. She is also part of the Karlsruhe School of Optics and Photonics (KSOP) and the 3DMM2O cluster (Thrust A1), completing the MBA Fundamentals program.



Aleksandra Vranic received her B.Sc. and M.Sc. degrees in Chemistry from the Karlsruhe Institute of Technology (Germany). She is currently working on her Ph.D., focusing on developing novel photoinitiators for 3D laser nanoprinting in Prof. Stefan Bräse's group, founded by the Karlsruhe School of Optics and Photonics (KSOP). She is also part of the 3DMM2O Cluster (Thrust A3).



Stefan Bräse studied in Göttingen (Germany), Bangor (U.K.), and Marseille (France), and received his Ph.D. in 1995 with Armin de Meijere in Göttingen. After postdoctoral research at Uppsala University and the Scripps Research Institute, he began his independent research career at the RWTH Aachen in 1997. In 2001, he finished his habilitation and moved to the University of Bonn as a professor of organic chemistry. Since 2003, he has been a professor at the Institute of Organic Chemistry, Karlsruhe Institute of Technology (KIT) and since 2012, also Director of the Institute of Biological and Chemical Systems – Functional Molecular Systems (IBCS-FMS) at the KIT. His research interests include chiral ligands and catalyst design for asymmetric processes, molecular engineering of functional synthetic materials and digitalization in chemistry.